eLife

Reviewed Preprint
v3 • August 12, 2025
Revised by authors

Reviewed Preprint
v2 • June 19, 2025

Reviewed Preprint
v1 • August 20, 2024

Microbiology and Infectious Disease

Spatial integration of sensory input and motor output in *Pseudomonas aeruginosa* chemotaxis through colocalized distribution

Zhengyu Wu, Maojin Tian, Sanyuan Fu, Min Chen, Rongjing Zhang, Junhua Yuan

Research Center of Translational Medicine, Central Hospital Affiliated to Shandong First Medical University, Jinan, China • Hefei National Research Center for Physical Sciences at the Microscale and Department of Physics, University of Science and Technology of China, Hefei, China • Research Center of Translational Medicine, Jinan Central Hospital, Shandong University, Jinan, China • Department of Critical Care Medicine, Zibo Central Hospital Affiliated to Binzhou Medical University, Zibo, China

eLife Assessment

This **important** study by Wu et al presents **convincing** data on bacterial cell organization, demonstrating that the two structures that account for bacterial motility - the chemotaxis complex and the flagella - colocalize to the same pole in Pseudomonas aeruginosa cells, and expose the regulation underlying their spatial organization and functioning. This manuscript will be of interest to cell biologists, primarily those studying bacteria.

https://doi.org/10.7554/eLife.97514.3.sa4

Abstract

The opportunistic pathogen *Pseudomonas aeruginosa* serves as a model organism for studying multiple signal transduction pathways. The chemoreceptor cluster, a core component of the chemotaxis pathway, is assembled from hundreds of proteins. The unipolar distribution of receptor clusters has long been recognized, yet the precise mechanism governing their assembly remains elusive. Here, we directly observed the relative positions of the flagellar motor and chemoreceptor cluster using flagellar filament labeling and gene editing techniques. Surprisingly, we found that both are located at the same cell pole, with the distribution pattern controlled by the polar anchor protein FlhF. Additionally, the efficient assembly of the chemoreceptor cluster is partially dependent on the integrity of the motor structure. Furthermore, we discovered that overexpression of the chemotaxis regulatory protein CheY leads to high intracellular levels of the second messenger c-di-GMP, triggering cell aggregation. Therefore, the colocalization of the chemoreceptor cluster and flagellum in *P. aeruginosa* serves to avoid cross-pathway signaling interference, enabling cells to conduct various physiological activities in an orderly manner.

Introduction

In biological systems, the process by which proteins self-assemble into organized complex structures is widespread[1,2]. Pole-to-pole protein oscillations in the *Min* system ensure that the FtsZ ring, a crucial component of cell division, is placed precisely in the middle of the cell body[3,4]. In response to antibiotic treatment and heat stress, some bacteria generate multiple protein foci throughout the cytoplasm[5,6]. The polar localization of the secretion system, such as the type [secretion system, is mediated by targeting proteins and potentially facilitates host-pathogen interactions[7,8]. Thus, spontaneous assembly is accompanied by the formation of spatial patterns that organize the intracellular environment.

To grow and colonize in various ecological niches, bacteria have evolved a mechanism for migrating towards more favorable environments. The locomotion organ (the flagellar motor) and the chemotaxis pathway play crucial roles in achieving this goal. The former provides physical drive, while the latter offers directional guidance. The initiation of cell reorientation is controlled by motor switching, which is governed by the chemotaxis two-component signaling pathway. This pathway comprises transmembrane chemoreceptors, a histidine kinase CheA, an adaptor protein CheW, a response regulator CheY, and two adaptation proteins, CheB and CheR. Receptors collaborate with CheA and CheW to form chemotaxis complex in a hexagonal pattern[9,10]. Upon phosphorylation of CheY by the kinase at the complex, it freely diffuses to the motor and binds to FliM, a component of the motor switch complex, to affect motor switching[11–13]. It is worth noting that there exists diversity among different bacterial species in the placement of flagellar motors[14], whereas chemoreceptor clusters are typically found at one or both ends of the cell[15]. These two structural units are functionally connected. However, it remains unclear whether there is an interaction in their spatial distribution and what the specific regulatory mechanism might be.

Pseudomonas aeruginosa, a common human opportunistic pathogen, possesses four chemosensory pathways that perform distinct functions and are stimulated by signal binding to 26 chemoreceptors[16]. Among them, the proteins encoded by chemotaxis-related genes collectively constitute the F6 pathway. Previous studies have suggested that the receptors involved in this pathway localize to the old cell pole[17], similar to the flagellum[18], implying colocalization of the receptors and the flagellum at the same pole; however, direct evidence for this colocalization is still lacking. Furthermore, the polar anchor protein FlhF has been reported to guide the flagellum to grow at the cell pole[19,20]. However, the mechanism by which chemotaxis complex-related proteins aggregate and self-assemble at the cell pole is controversial. The distribution of the chemotaxis complex in the peritrichous bacterium *Escherichia coli* has been extensively studied and attributed to several mechanisms, including stochastic self-assembly[21,22], membrane curvature sorting[23,24], and inefficient clustering in the lateral region[25]. However, these mechanisms cannot explain the unipolar distribution pattern observed in *P. aeruginosa*. Unlike *E. coli*, specific genes responsible for the placement of the chemotaxis complex have been identified in several bacterial species. In *Caulobacter crescentus*, chemotaxis complex assemble at the new cell pole with the help of TipN and TipF proteins[26]. A tripartite ParC-ParP-CheA interaction network was reported to promote polar localization of chemotaxis complex in *Vibrio parahaemolyticus*[27,28]. However, as there are no related genes in *P. aeruginosa*, the mechanism of its chemotaxis complex distribution remains a mystery.

Here, we combined gene editing and in vivo fluorescence imaging of flagellar filaments to directly observe the distribution of chemotaxis complex and flagellar motors, proposing a cooperative construction model of chemotaxis network and flagella during the entire division cycle of *P. aeruginosa*. The core focus of this study is to clarify the regulatory mechanism of its chemotaxis complex distribution. We found a substantial association between the assembly of the flagellar

motor and the chemotaxis complex. The assembly efficiency of the receptor complex is influenced by core flagellar motor components, particularly the C-ring and MS-ring structures, while its assembly site is also affected by the polar anchor protein FlhF. Furthermore, by introducing exogenously expressed CheY protein, we found that this triggers the expression of c-di-GMP at a high level. From this, we infer that the colocalization of the chemotaxis complex and the flagellum in *P. aeruginosa* avoids the cross-pathway interference of signaling molecules, thus providing a guarantee for the coexistence of multiple chemosensory pathways.

Results

Robust generation of daughter cell with both chemotaxis network and flagellar motor

CheY has been shown to colocalize with chemoreceptors[17,29]. To visualize the distribution of chemotaxis complex in cells, we fused the gene encoding the enhanced yellow fluorescent protein (eYFP) to the *cheY* gene in the *P. aeruginosa* chromosome (**Fig. 1A**). All genetic modifications were carried out at the native position on the chromosome, allowing the expression of chemotaxis proteins in precise stoichiometry from their natural promoters (**Fig. 1B**). The mutant strain with *cheY-eyfp* was able to moderately expand on soft agar plates[17], proving that its chemotaxis behavior was not notably affected, so it was selected for subsequent experiments. As shown in **Fig. 1C**, CheY-eYFP was mainly located at the cell pole, suggesting that CheA, CheW and CheY in *P. aeruginosa* form a signal transduction complex that was primarily distributed at the cell pole, as described previously[17]. Representative large-field images containing many cells are shown in Fig. S1. Additionally, we constructed a plasmid expressing CheA-CFP and electroporated it into the *cheY-eyfp* strain. Fluorescence imaging revealed a high degree of spatial overlap between CheA-CFP and CheY-EYFP (Fig. S2), confirming that CheY-EYFP accurately marks the location of the chemoreceptor complex. From our measurements, nearly 90% (332/372) of cells contain obvious receptor clusters, and factors such as fluorescence bleaching may have caused the loss of fluorescent spots in some cells. In addition, we observed the presence of fluorescent spots at both ends of some cells with a large aspect ratio (probably approaching cell division), indicating that the newly generated progeny cells will have a complete chemotaxis network. Next, we sought to observe the distribution of the flagella in cells simultaneously to understand the motility of future progeny.

Our recent study demonstrated the successful labeling of the flagellar filament with thiol-reactive fluorescent dye by introducing cysteines into the flagellin FliC[30,31] (**Fig. 1B**). To avoid fluorescence interference, we utilized a dye with an excitation peak near 568 nm, considering that the excitation peak of eYFP is 513 nm, and the emission peak is 527 nm. We employed a xenon lamp as the excitation light source and switched filters to enable simultaneous fluorescence imaging of flagellar filaments and chemotaxis complex within the same cell.

Remarkably, our findings revealed a surprising colocalization of chemotaxis complex and flagellar filaments at the same end of the cell body, and this colocalization was consistent, as shown in **Fig. 1D**. A typical large field was shown in Fig. S3. Similar to the chemotaxis complex, we observed the phenomenon of double flagella symbiosis in cells with a large aspect ratio, suggesting that *P. aeruginosa* has evolved a cell division mechanism with precise timing regulation. Before cell division, both poles of the mother cell assembled chemotaxis complex and flagellar motors. This ensures that daughter cells possess complete motility and chemotaxis, thereby greatly enhancing the environmental adaptability of the population.

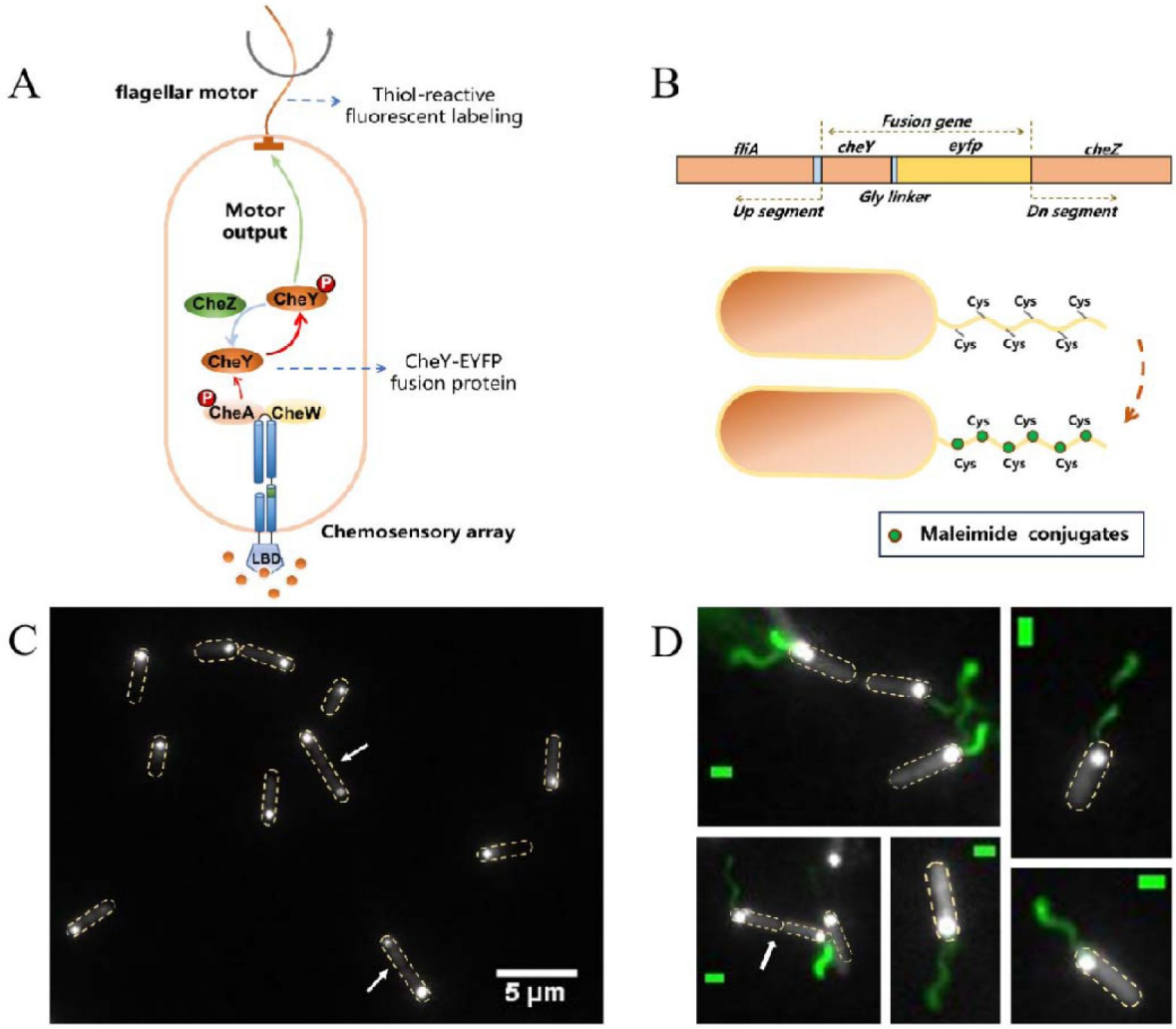

Fig. 1.

A. Schematic diagram of the chemotaxis signal transduction network and flagellar motor of *P. aeruginosa*. Fusion protein CheY-EYFP and fluorescently labeled flagellar filaments were used as markers to indicate the position of the chemotaxis complex and motor, respectively. **B.** The labeling mechanism of flagellar filaments and chemotaxis regulatory protein CheY. Filaments (with cysteine point mutation $FliC^{T394C}$) were labeled through sulfhydryl-maleimide conjugation, and *cheY-eyfp* fusion with a 3× glycine linker was used to visualize chemotaxis complex positions. **C.** Localization of CheY-EYFP in the wild-type strain of *P. aeruginosa*. CheY-EYFP is mainly located at the single cell pole, and the white arrow points to individuals with obvious chemotaxis complex at both cell poles, which generally have a large aspect ratio of the cell body. The yellow dashed box marks the cell outline. **D.** The merged imaging of flagellar filaments and CheY-EYFP in the wild-type strain of *P. aeruginosa*, where flagellar motor and chemotaxis complex colocalize in cells. 145 cells with labeled flagella were observed, all of which exhibited consistent colocalization. White arrows point to individuals about to be divided, and the yellow dashed box marks the cell outline. The scale bar is 1 μm.

FlhF controls polar targeting but not flagellum-chemoreceptor colocalization

Despite potential differences in the physical and especially physiological environments at the two cell poles, it is unlikely that the unipolar distribution of the chemotaxis complex can be attributed to passive regulatory factors. The number and distribution of flagellar motors and chemotaxis complex vary among different bacterial species[14,15], and the localization system for flagella has been well studied. Specifically, the FlhF-FlhG system, discovered in several monotrichous bacterial species, has been shown to control the location and number of flagella[32,33]. In *P. aeruginosa*, a knockout of *flhF* leads to mis-localized flagellar assembly[19,20]. Considering the consistent colocalization pattern between chemotaxis complex and flagellar motors in *P. aeruginosa*, we speculate that the distribution of chemotaxis complex is also regulated by similar molecular mechanisms.

To investigate the role of FlhF in the localization of chemotaxis complex, we constructed a Δ*flhF* strain for fluorescence observation. The results revealed that the chemotaxis complex no longer grow robustly at the cell pole (**Fig. 2A**), and the assembly positions of the flagellar motor change accordingly, colocalizing with the chemotaxis complex (**Fig. 2B**). Representative large fields containing many cells are shown in Fig. S1. Additionally, we categorized receptor cluster distribution patterns into three types: precise polar, near polar, and mid-cell. We artificially divided the intracellular area along the long axis of the cell. The two ends of the length accounted for 10% each, which we called the precise-polar domains, the middle 50% became the mid-cell domain, and the rest was called the near-polar domain. The type of complex distribution was determined by the partition where the center of the chemotactic complex fluorescent bright spot was located. The relevant statistics for the wild-type strain and the Δ*flhF* mutant are presented in Fig. S4, showing that the proportion of precise polar distribution of chemotactic complexes decreased by 12.8% after *flhF* knockout. We also quantified the proportion of individuals with obvious receptor clusters, which was more than 80% (182/221), similar to the wild-type strain. These experimental results suggest that the polar anchoring protein FlhF has a minimal impact on the assembly efficiency of *P. aeruginosa*'s chemotaxis complex, but it affects its unipolar distribution. Furthermore, a consistent colocalization between the flagellar motor and chemotaxis complex was observed, independent of FlhF. Thus, it is crucial to determine whether there is a causal relationship in the assembly order of these two structural units.

Core motor structures influence chemoreceptor complex assembly

Cryo-electron microscopy has successfully revealed the complete flagella structure in various bacterial species. This structure includes multiple components such as the inner-membrane MS ring, the cytoplasmic C ring, and the internal protein secretion system, all of which exhibit strong similarities[34]. This suggests that the core structure of the flagellar motor is highly conserved. The MS ring, composed of 26 FliF proteins, forms the foundation of the flagellar structure[35]. In addition to serving as a mounting platform for the C ring, the MS ring also acts as a protective shell for the internal protein secretion machinery[36]. FliG, the main component protein of the C ring, binds directly to the cytoplasmic surface of FliF in a 1:1 ratio[37]. Thus, the efficient assembly of the C ring requires preassembly of the MS ring. To observe the distribution of the chemotaxis complex following the disruption of the C ring and MS ring, we constructed Δ*fliG* and Δ*fliF* mutants.

We performed fluorescence observation on the Δ*fliG* mutant, which has a disrupted flagellar motor C ring. The results showed that the proportion of Δ*fliG* cells with obvious chemoreceptor clusters decreased significantly compared to the wild-type cells (59.8%, 140/234), although the chemotaxis complex remained at a single cell pole. We also examined the Δ*fliF* mutant, which has a disrupted flagellar motor MS ring. Similar to the Δ*fliG* mutant, the proportion of individuals with

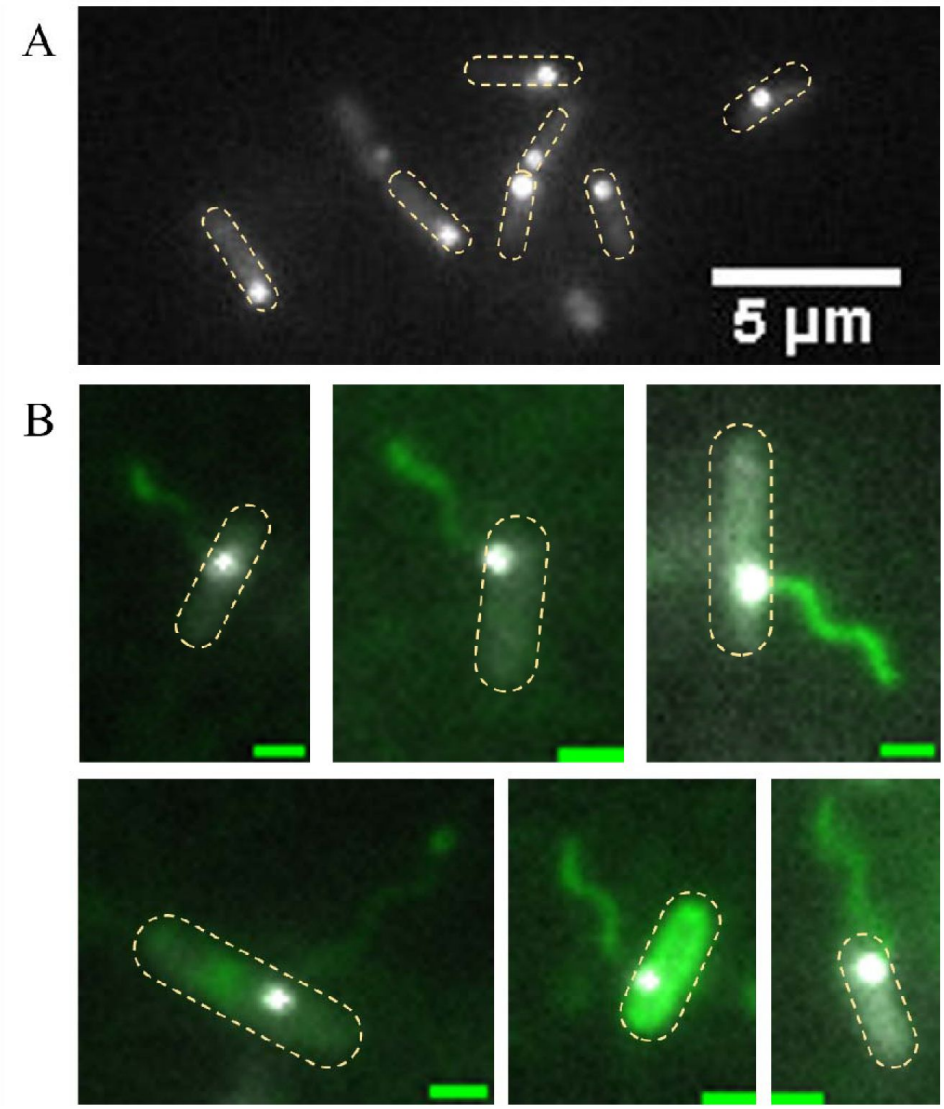

Fig. 2.

A. Localization of CheY-EYFP in the Δ*flhF* strain of *P. aeruginosa*. CheY-EYFP is no longer robustly distributed at the single cell pole. The yellow dashed box marks the cell outline. **B.** The merged imaging of flagellar filaments and CheY-EYFP in the Δ*flhF* strain of *P. aeruginosa*, flagellar motor and chemotaxis complex still colocalize in cells. 101 cells with labeled flagella were observed, all of which exhibited consistent colocalization. The yellow dashed box marks the cell outline. The scale bar is 1 μm.

obvious chemotaxis complex decreased significantly (62.5%, 202/323). Subsequently, we constructed a Δ*flhF*Δ*fliF* mutant and observed that the proportion of individuals with obvious chemoreceptor clusters further decreased (50.7%, 341/672). To ascertain whether it is motor integrity rather than functionality that influences the efficiency of chemotaxis complex assembly, we constructed a stator mutant (Δ*motA*Δ*motCD*). In this mutant, the motor is completely stalled while the structure remains intact. We found that the mutant performed similarly to the wild-type strain in terms of chemotaxis complex assembly (84.3% of individuals with obvious clusters, 204/242). The fluorescence imaging of receptor clusters for multiple mutants in this section is shown in **Figure. 3A**, and corresponding large-field images are provided in Fig. S1. We utilized Western blotting to measure the expression levels of CheY, which were found to be similar across the different strains (**Fig. 3B**). These further substantiated that the observed phenomenon is based on the structural integrity of the motor rather than the protein expression level. In contrast, the *cheA* knockout strain was constructed to disrupt the assembly of the chemoreceptor complex. We fluorescently labeled its flagellar filaments and found that its phenotype was no different from that of the wild-type strain (Fig. S5), indicating that the assembly of the chemotactic receptor complex does not affect the flagellar assembly efficiency. The P ring (mainly composed of FlgI) is thought to act as a bushing for the peptidoglycan layer, and its absence results in partial assembly of the motor structure[38]. We constructed Δ*flgI* mutant and found that the proportion of cells with distinct chemotactic complexes was similar to that of the wild-type (Fig. S6). Additionally, we quantified the proportion of cells with receptor clusters (**Fig. 3C**). Overall, our findings suggest that the polar anchor protein FlhF and the structural integrity of the motor are crucial for the formation of chemotaxis complex. The former guides them to the appropriate site, while the latter influences the assembly efficiency of the chemoreceptor complex.

Colocalization of chemotaxis complex and flagellar motor avoids cross-pathway interference in *P. aeruginosa* signal transduction

The distribution patterns of receptors associated with various signal transduction pathways in *P. aeruginosa* vary considerably. For instance, the biofilm formation-related receptor WspA, unlike the chemotaxis receptors discussed here, is distributed throughout the cell. This distribution is thought to enhance its sensitivity to mechanical perturbations of the cell membrane[39]. Previous studies speculated that the highly consistent position of chemotaxis complex and flagellar motors enhances bacterial chemotaxis performance[28]. However, the diffusion time of the phosphorylated chemotaxis regulatory protein CheY-P across the longest distance in a bacterial cell body (along the cell's long axis) is approximately 100 ms[40,41], whereas the timescale for the chemotaxis temporal comparison is on the order of seconds[42]. Additionally, a study by Fukuoka and colleagues reported that intracellular chemotaxis signal transduction requires approximately 240 ms beyond CheY or CheY-P diffusion time[41]. Moreover, the CCW/CW interval of the *P. aeruginosa* flagellar motor under normal conditions is 1-2 s, as determined by bead assays[30] or tethered cell assays[43]. Taken together, these indicate that for *P. aeruginosa*, which moves via a run-reverse mode, the potential 100 ms reduction in response time due to co-localization of the chemotaxis complex and motor has a limited effect on overall chemotaxis timing. Consequently, the physiological significance of the colocalization of chemoreceptors and flagellar motors remains unclear.

E. coli mediates chemotaxis through a single pathway involving five types of chemoreceptors[44]. As a core regulatory protein for chemotaxis, CheY participates in multiple processes such as adaptation and chemotaxis response, with CheY-P binds to the motor to regulate switching[11]. In contrast, *P. aeruginosa* has four distinct chemosensory pathways that perform different functions, involving different CheY homologs, and are stimulated by signals binding to 26 types of chemoreceptors. Consequently, *P. aeruginosa* possesses more complex chemosensory pathways[16]. We thus hypothesized that the co-localization of chemoreceptors and flagellar

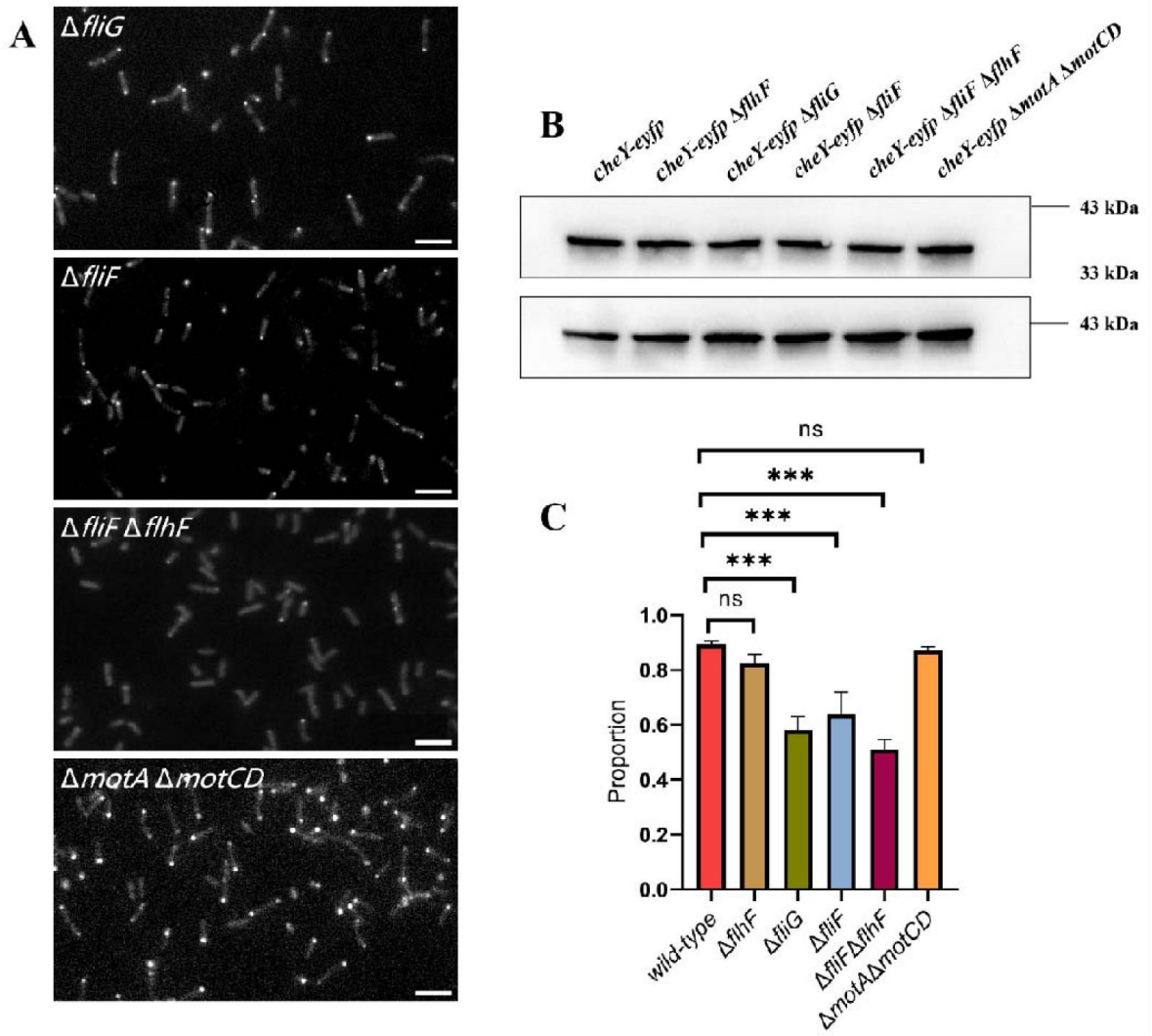

Fig. 3.

A. Localization of CheY-EYFP in various *P. aeruginosa* strains. The scale bar is 10 μm. **B.** Western blot analysis was performed to detect CheY expression in various *P. aeruginosa* strains. β-actin was used as the housekeeping protein. **C.** Occurrence probability of obvious chemotaxis complex in *P. aeruginosa* wild-type and several mutant strains. The proportion of individuals with obvious chemotaxis complex decreased significantly in the motor-incomplete strains (Δ*fliF* and Δ*fliG*), and this value was further reduced after *flhF* knockout (Δ*fliF*Δ*flhF*). The Δ*fliF* and Δ*motA*Δ*motCD* strains have a similar chemotaxis complex occurrence probability as the wild-type strain. The number of cells analyzed for each strain (from left to right) were: 372, 221, 234, 323, 672, and 242. '***': significant difference (P-value < 0.0001), 'ns.': no significant difference (P-value > 0.05).

motors in *P. aeruginosa* ensures locally distributed CheY-P molecules, thereby eliminating the need for a high level of intracellular CheY-P and avoiding potential side effects on other signaling pathways.

To test the potential effect of an increased intracellular CheY-P level, we constructed the CheY expression plasmid *cheY*-pJN105, transformed it into the wild-type *P. aeruginosa* strain, and induced it with varying concentrations of arabinose. We observed that the higher the inducer concentration, the more pronounced the cell aggregation became in the field of view (**Fig. 4A**). The transition from planktonic individuals to aggregated communities is similar to biofilm formation, which is known to be accompanied by a significant increase in intracellular c-di-GMP levels.

To investigate whether a higher level of intracellular CheY-P increased the intracellular c-di-GMP level, we sought to detect the c-di-GMP level. We introduced the plasmid pCdrA-gfp into *P. aeruginosa*, using it as a c-di-GMP biosensor with the fluorescence intensity proportional to the c-di-GMP level[45]. To ensure the coexistence of the plasmids, the intracellular CheY concentration was controlled by the plasmid *cheY*-pME6032. The intracellular CheY levels induced by varying arabinose concentrations were measured, showing clear differences across the concentration gradient (Fig. S7). We found that the average single-cell fluorescence intensity of the CheY overexpression strain was 71.8% higher than that of the wild-type strain, while the c-di-GMP level of the *cheY* deletion strain was 58.6% lower than that of the wild-type (**Fig. 4B**).

The colocalization of both the signaling source (the kinase) and sink (the phosphatase) at the chemoreceptor complex at the cell pole results in a rapid decay of CheY-P concentration within approximately 0.2 μm from the cell pole, leading to a nearly uniform distribution elsewhere in the cell, as demonstrated by Vaknin and Berg[46]. This spatial arrangement effectively confines high CheY-P levels to the pole region. When the motor is also localized at the cell pole, the need for elevated CheY-P concentrations throughout the cytoplasm is reduced. Therefore, the colocalization of chemotaxis complex and flagellar motor facilitates the precise regulation of cell swimming direction within the low intracellular CheY-P concentration threshold, using locally distributed CheY-P molecules. This helps to avoid the occurrence of the aforementioned cross-pathway interference. To further confirm that CheY overexpression promotes aggregation through increased c-di-GMP levels, we performed additional experiments co-overexpressing CheY and a phosphodiesterase (PDE) from *E. coli* to reduce intracellular c-di-GMP. These experiments showed that PDE expression mitigates cell aggregation caused by CheY overexpression in *P. aeruginosa* (Fig. S8).

Summary and Discussion

P. aeruginosa harbors multiple signal transduction systems that regulate flagella-mediated swimming motility (Che pathway), pili-mediated interface twitching motility (Pil pathway), and biofilm formation (Wsp pathway)[16]. These systems allow it to thrive in various ecological niches within complex external environments. Here, employing a combination of chromosomal fluorescent protein fusion and flagellar labeling techniques in living cells, we directly observed that the chemotaxis complex of *P. aeruginosa* Che pathway and the flagellar motor share a high degree of consistency in their assembly sites. We found that the chemotaxis complex, comprising Che proteins, was consistently located at the cell pole where the flagellum was positioned. Based on these observations, we deduced the construction mode of the chemotactic network and flagellar motor during the entire cell growth cycle (**Fig. 5A**). As the cell body matures and elongates, a new flagellum grows at the opposing cell pole, accompanied by the assembly of a fresh chemotaxis complex. The cell then undergoes division from the middle, generating two daughter cells, each equipped with fully functional motility and chemotaxis capabilities. This ensures robust inheritance of these chemotaxis and motility-related macromolecular machines.

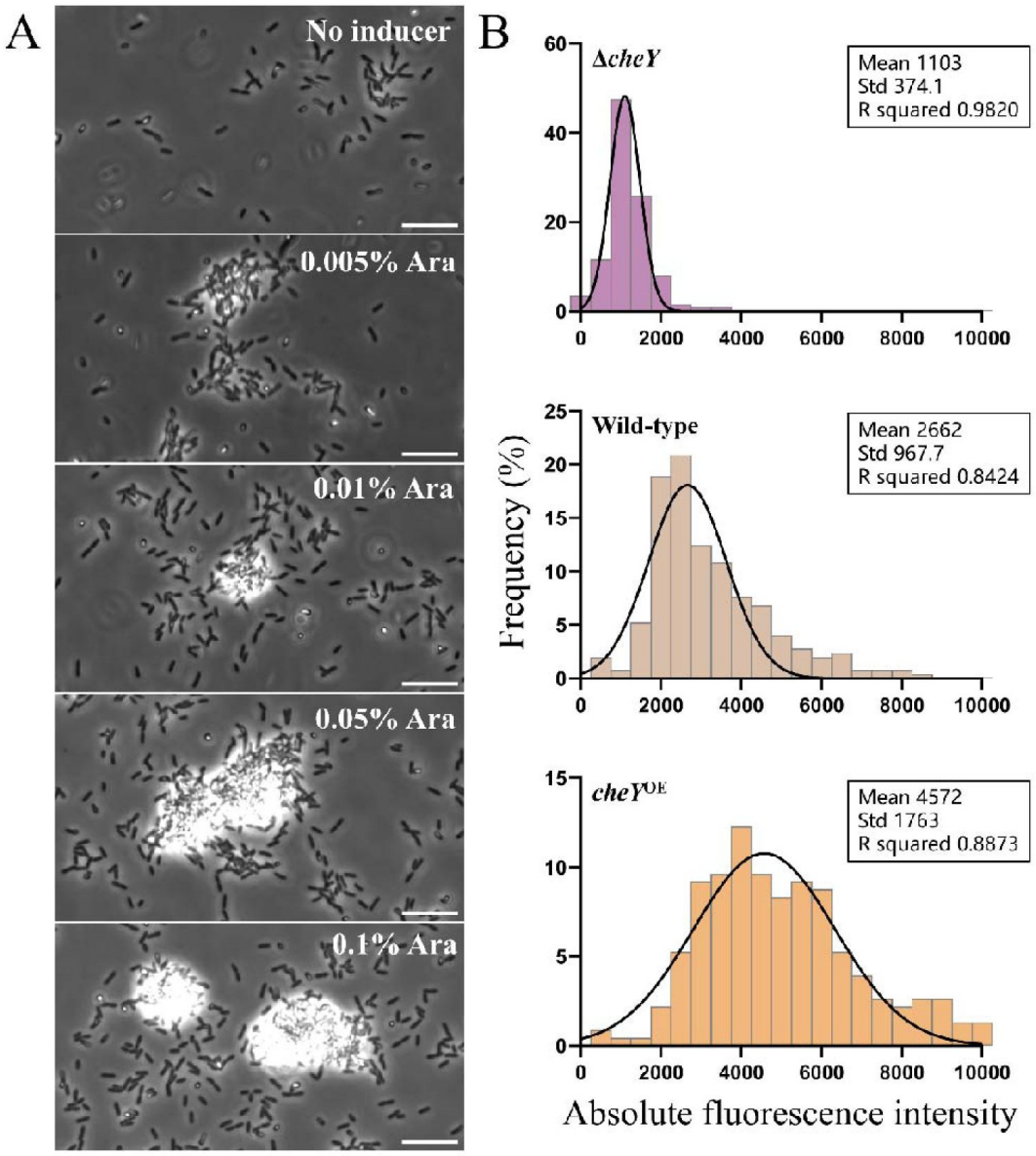

Fig. 4.

A. The evolution of cell aggregation as the intracellular CheY concentration increases by induction with higher concentrations of arabinose. The scale bar is 10 μm. **B.** Quantitative characterization of intracellular c-di-GMP levels at different CheY concentrations. From top to bottom, they correspond to the Δ*cheY* strain (N=198), wildtype strain (N=249) and CheY overexpression strain (N=228), respectively.

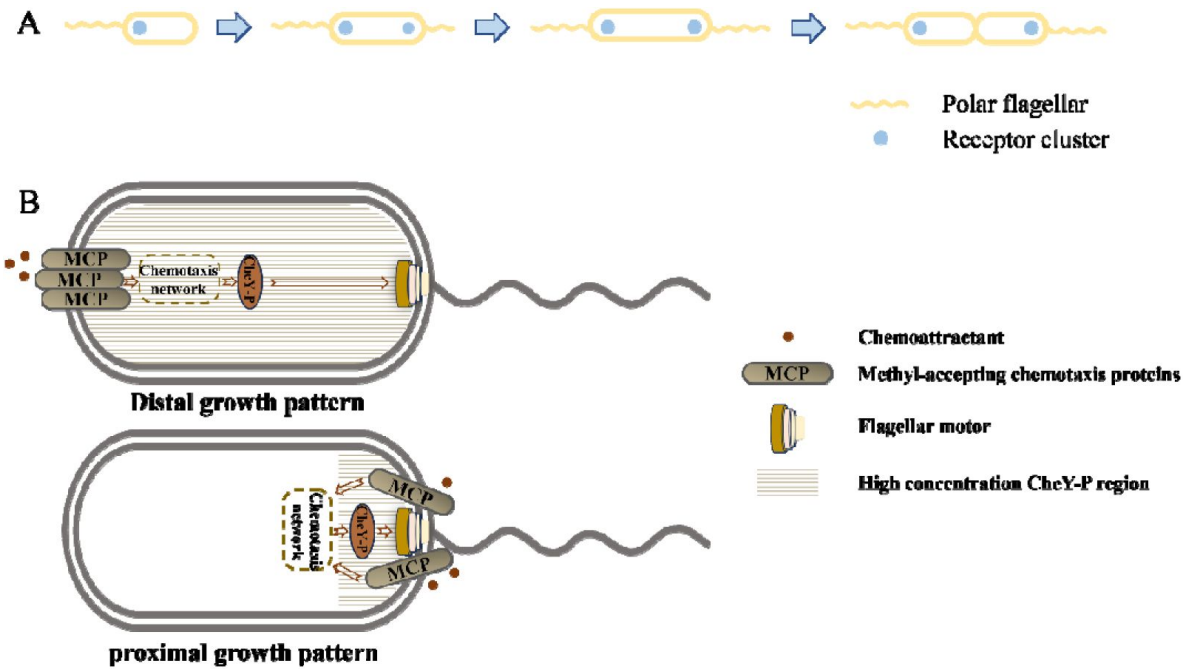

Fig. 5.

A. The construction mode of the chemotaxis network and flagellar motor throughout the complete cell growth cycle. **B**. The proximal growth mode of the *P. aeruginosa* flagellar motor and receptor clusters will effectively regulate the spatial range of CheY action, thus avoiding unintentional cross-pathway regulation.

Based on our understanding of the regulation mechanism of flagellar position in *P. aeruginosa*, we constructed a Δ*flhF* mutant and found that the position distribution of its chemotaxis complex is actively regulated by FlhF-mediated molecular mechanisms, rather than being passively restricted by membrane curvature factors as seen in *E. coli*. A similar active regulation phenomenon was previously reported in *Vibrio cholerae*, with the corresponding molecular regulation mechanism detailed extensively[28]. The flagella and chemotaxis complex of newborn *V. cholerae* cells are located at the old cell pole, with the polar anchor protein HubP distributed at both cell poles. As the cell grows, HubP recruits the ParA homologue ParC. Subsequently, ParC recruits ParP to assemble a new chemotaxis complex at the new cell pole. Upon cell division, HubP relocates to the middle of the cell, ensuring its robust presences at both poles of the daughter cells. Here, HubP recruits ParA homologues including FlhG, which influence flagellar motor assembly. However, previous experiments confirmed that the cell cycle-dependent polar localization of ParC and chemotactic proteins is independent of the flagellar position regulatory protein FlhF. This suggests that the localization of flagellar motors and chemotaxis complex in *V. cholerae* is controlled separately through different pathways. In contrast, flagellar motors were no longer robustly distributed at the cell pole after *flhF* was knocked out in *P. aeruginosa*, whereas the assembly site of chemotaxis complex and flagellar motor remained remarkably consistent. This suggests that FlhF regulates the distribution patterns of both and implies an interaction between them.

We further constructed Δ*fliG* and Δ*fliF* mutants, which disrupted the assembly of the flagellar motor. Surprisingly, we observed that the assembly of chemotaxis complex was impaired under these conditions, with a significant decrease in the proportion of individuals exhibiting obvious Che protein fluorescent bright spots. In contrast, the chemotaxis complex assembly in the stator mutant (Δ*motA*Δ*motCD*) was similar to that of the wild-type strain. It should be noted that *P. aeruginosa* has a four-tiered transcriptional regulatory circuit controlling flagellar biogenesis, in which FliG and FliF belong to class II and are regulated by the master transcriptional regulator FleQ[47]. Chemotaxis complex-related genes (*cheA*, *cheW*, etc.) are regulated by intracellular free FliA proteins. In *E. coli*, FliA is bound and inhibited by FlgM, and upon hook assembly, FlgM is secreted outside the cell, allowing FliA to trigger transcription of class III genes[48,49], which include the chemosensory genes. This implies that if the hook is not assembled, late genes (including chemoreceptors) should not be expressed. However, Kaplan et al. reported that chemotaxis complexes were observed in *Shewanella oneidensis* Δ*fliF* mutant[50], suggesting a different assembly process from that of *E. coli*. We therefore investigated whether knocking out *fliF* or f*liG* affects the expression level of *che* genes in *P. aeruginosa*. Since most experiments in this study focused on CheY, we performed Western blotting to measure CheY expression levels in wild-type, Δ*fliF* and Δ*fliG* strains, and found no significant differences (**Fig. 3B**). These results suggest that the observed decrease in the proportion of chemotaxis complexes after knocking out *fliF* and *fliG* should be attributed to the lack of motor assembly rather than changes in Che protein expression levels. To eliminate the potential confounding effects of FlhF and flagellar motors, we constructed a Δ*flhF*Δ*fliF* mutant strain. Under this condition, the proportion of individuals with obvious Che protein fluorescent bright spots dropped to ~50%, indicating that passive regulation based on membrane curvature may still exist in *P. aeruginosa*, albeit to a lesser degree.

Is the remarkable consistency in the spatial distribution of these two independent structural units an unintentional outcome or a hidden mystery? Given that Kulasekara et al. previously proposed that CheA and its phosphorylation state can cause c-di-GMP heterogeneity among individual *P. aeruginosa* cells through a specific PDE[51,52], we sought to verify whether the phenotypic differences induced by CheY here are closely related to changes in the overall population level of c-di-GMP. We introduced a c-di-GMP monitoring system at the single-cell level and discovered that overexpression CheY substantially increases the intracellular c-di-GMP concentration. Previous studies generally believed that CheY-P, as a chemotactic regulatory protein, only influences flagellar motor switching. Here, we found that CheY-P, as a signaling molecule, can accomplish threshold-limited cross-pathway regulation. At low CheY-P concentrations, it is conservatively involved in motor switching regulation, as confirmed by previous studies. At high CheY-P

concentrations, cell motility is suppressed, and c-di-GMP is triggered to express, though its specific mechanism needs further exploration. Unlike CheA, a structural protein of the chemotaxis complex, CheY is a protein that can shuttle in the cytoplasm and can also regulate the intracellular c-di-GMP level. This finding expands our understanding of the connection between the internal chemotaxis network and the c-di-GMP pathway. The intracellular environment is highly crowded[53], and the proximal growth pattern shown in **Fig. 5B** has multiple physiological significances. On one hand, chemotaxis-related protein can precisely regulate cell motility with minimal synthesis costs. On the other hand, the chemotactic network and the flagellar motor are spatially integrated within the cell, ensuring their robust existence within the cell body and preventing mutual interference with collateral pathways.

Many bacteria possess multiple signal transduction pathways. The orderly operation of each pathway within the micrometer-scale space presents a fascinating scientific problem. Here, we utilized the well-known chemotaxis network as a starting point to shed light on this problem, providing inspiration for future in-depth understanding of related issues.

Materials and methods

Strains and cell culture

The strains and plasmids used in this study are listed in **Table 1**. The *Escherichia coli* TOP10 strain was used for standard genetic manipulations. A single-colony isolate was grown in 3 ml of LB broth (1% Bacto tryptone, 0.5% yeast extract and 1% NaCl) overnight to saturation on a rotary shaker (250 rpm) at 37°C. An aliquot was diluted 1:100 into 10 ml of LB broth and grew to exponential phase. Appropriate antibiotics were added if necessary to prevent plasmid loss: for *E. coli*, 15 μg/ml Gentamicin and 25 μg/ml Tetracycline; for *P. aeruginosa*, 30 μg/ml Gentamicin and 50 μg/ml Tetracycline. To induce protein expression, Isopropyl β-D-1-thiogalactopyranoside (IPTG, 1.0 mM) was added to strains with pME6032-derivative vectors, and arabinose (0.005%, 0.01%, 0.05%, 0.1%) was added to strains with pJN105-derivative vectors. 2 ml of cells were harvested by centrifugation at 2000×*g* for 2 min, washed twice in an equal volume of motility buffer (MB) [50 mM potassium phosphate, 15 μM EDTA, 0.15 M NaCl, 5 mM Mg^{2+} and 10 mM lactic acid (pH 7.0)][54], and resuspended in 5 ml MB for subsequent fluorescence observation.

Construction of in-frame deletion mutants

We used polymerase chain reaction (PCR) to generate ~1000 bp DNA fragments with upstream (Up) and downstream (Dn) sequences flanking the target gene (including *flhF*, *fliF*, *motA* and *fliG*) to be deleted. The Up and Dn DNA sequences were fused with the linearized pex18gm vector using Gibson assembly[55]. The resulting vectors were transformed into *P. aeruginosa* by electroporation, and the desired knockout mutants were obtained by double selections on gentamicin plates (LB plates with 30 μg/ml gentamicin) and sucrose plates (NaCl-free LB plates with 15% sucrose) at 37°C[56].

Generation of chromosomal fusions of *yfp* to *P. aeruginosa* gene

To generate *eyfp* fusion at the N-terminus of *cheY*, we first used PCR to generate upstream and downstream DNA sequences flanking the *cheY* gene. A subsequent PCR reaction aimed to yield the *cheY-eyfp* fusion with a 3× glycine linker (GGCGGAGGA), with pVS88 serving as the source of the enhanced yellow fluorescent (*eyfp*). The three DNA sequences, along with the linearized vector, were fused to *cheY-eyfp*-pex18gm using Gibson assembly. Finally, gene replacement was used to transfer the fusion constructs into the *P. aeruginosa* chromosome by homologous recombination.

Strain, Plasmid	Genotype, phenotype, and Description	Source
Strains		
P. aeruginosa		
PAO1	wild-type strain	Fan Jin Group
PAO1 *fliC*^{T394C}	Replacement of chromosomal *fliC* in PAO1	Ref 31
PAO1 *fliC*^{T394C} *cheY-eyfp*	*yfp* fusions at the N-terminus of *cheY* in PAO1 *fliC*^{T394C}	This work
PAO1 *fliC*^{T394C} *cheY-eyfp* Δ*flhF*	Nonpolar *flhF* deletion in PAO1 *fliC*^{T394C} *cheY-eyfp*	This work
PAO1 *fliC*^{T394C} *cheY-eyfp* Δ*fliF*	Nonpolar *fliF* deletion in PAO1 *fliC*^{T394C} *cheY-eyfp*	This work
PAO1 *fliC*^{T394C} *cheY-eyfp* Δ*fliG*	Nonpolar *fliG* deletion in PAO1 *fliC*^{T394C} *cheY-eyfp*	This work
PAO1 *fliC*^{T394C} *cheY-eyfp* Δ*flhF* Δ*fliF*	Nonpolar *fliF* deletion in PAO1 *fliC*^{T394C} *cheY-eyfp* Δ*flhF*	This work
PAO1 *fliC*^{T394C} *cheY-eyfp* Δ*motA* Δ*motCD*	Nonpolar *motAB* and *motCD* deletion in PAO1 *fliC*^{T394C} *cheY-eyfp*	This work
PAO1 *fliC*^{T394C} Δ*cheA*	Nonpolar *cheA* deletion in PAO1 *fliC*^{T394C}	This work
PAO1 *fliC*^{T394C} *cheY-eyfp* Δ*flgI*	Nonpolar *flgI* deletion in PAO1 *fliC*^{T394C} *cheY-eyfp*	This work
E. coli		
Top10	F-*mcrA* Δ(*mrr-hsRMS-mcrBC*)Φ80*lacZ*Δ*M15* Δ*lacX74 recA1* *ara*D139 Δ(*araleu*)7697 *galU galK rpsL*(Nal^{R}) endA1 *nupG*	Invitrogen
Plasmids		
pex18gm	oriT^{-}sacB^{-}; gene replacement vector with MCS from pUC18; Gm^{r}	Fan Jin Group
flhF-pex18gm	In-frame deletion of *flhF* cloned into pex18gm; Gm^{r}	This work
fliF-pex18gm	In-frame deletion of *fliF* cloned into pex18gm; Gm^{r}	This work
fliG-pex18gm	In-frame deletion of *fliG* cloned into pex18gm; Gm^{r}	This work
motA-pex18gm	In-frame deletion of *motA* cloned into pex18gm; Gm^{r}	This work
motCD-pex18gm	In-frame deletion of *motCD* cloned into pex18gm; Gm^{r}	Ref 30
cheA-pex18gm	In-frame deletion of *cheA* cloned into pex18gm; Gm^{r}	This work
flgI-pex18gm	In-frame deletion of *flgI* cloned into pex18gm; Gm^{r}	This work
cheY-eyfp-pex18gm	*eyfp* fusions *cheY* cloned into pex18gm; Gm^{r}	This work
cheY-pJN105	*cheY* overexpression vector in pJN105, *cheY* expression is controlled by P_{BAD} promoter; Gm^{r}	This work
cheY-pME6032	*cheY* overexpression vector in pME6032, *cheY* expression is controlled by P_{lac} promoter; Tet^{r}	This work
ylxjH-pME6032	*ylxjH* overexpression vector in pME6032, *ylxjH* expression is controlled by P_{lac} promoter; Tet^{r}	This work
pCdrA-*gfp*	pUCP22-NotI based cyclic di-GMP level reporter, Gm^{r}	Ref 45
cheY-eyfp-pJN105	*eyfp* fusions *cheY* cloned into pJN105, *cheY-eyfp* expression is controlled by P_{BAD} promoter; Gm^{r}	This work
cheA-ecfp-pJN105	*ecfp* fusions *cheA* cloned into pJN105, *cheA-ecfp* expression is controlled by P_{BAD} promoter; Gm^{r}	This work

Table 1.

Strains and plasmids used in this study.

Flagellar staining and fluorescence imaging

Flagellar filaments were labeled by following the protocol described previously[57]. Cells (1 ml of exponential-phase culture) were harvested by centrifugation at 2000×*g* for 10 min and washed twice in 1 ml MB. The final pellet was adjusted to a volume of ~100 µl that concentrated the bacterial 10-fold. Alexa Fluor 568 maleimide (Invitrogen-Molecular Probes) was added to a final concentration of 20 µg/ml, and labeling was allowed to proceed for 30 min at room temperature with gyration at 80 rpm. Unused dye was then removed by washing the cells with MB three times, and the final pellet was resuspended in MB.

For fluorescence imaging, 50 µl of cells were added to the chamber (constructed with two double-sticky tapes, a glass slide, and a poly-L-Lysine coated coverslip), incubated for 3 min, and rinsed with 100 µl MB. The boundary of the chamber was then sealed with Apiezon vacuum grease. The chamber was placed on a Nikon Ti-E inverted fluorescence microscope with a 100× oil-immersion objective and a sCMOS camera (Primer95B, Photometrics). The flagellar filament and chemotaxis complex of cells were observed separately with corresponding filter-set, using a 200-ms exposure time. To quantify the fluorescence intensity of the receptor cluster, we took the intensity maximum point as the center and extract a 3×3 pixel matrix around it. The mean value of the elements in this matrix represents the final fluorescence intensity.

Western Blotting

The total protein of *P. aeruginosa* strain cells in each treatment group was extracted and its concentration was measured with Bicinchoninic acid (BCA Protein Quantification Kit, Yeasen Biotechnology Co., Ltd) when the cells grew to exponential phase with same reduced turbidity (OD_{600} between 0.9 and 1.0). The exact amount of protein was subjected to SDS-PAGE electrophoresis, then transferred to a nitrocellulose membrane, which was blocked with 50 mg/mL skim milk in TBST buffer (20 mM Tris, 150 mM NaCl [pH7.4], 0.1%Tween 20) for 1h at room temperature. Since the N-terminal sequence of EYFP is almost identical to that of GFP, a rabbit anti-GFP antibody (1:2000, Yeasen Biotechnology Co., Ltd) and a Mouse anti-β-actin antibody (1:2000, Invitrogen) were added and incubated at 4°C overnight. The nitrocellulose membrane was gently washed with TBST for 20 min, three times. Subsequently, HRP labeled goat anti-rabbit IgG (1:4000, Abcam) and rabbit anti-mouse IgG (1:4000, Abcam) were added and incubated at room temperature for 1 h. The nitrocellulose membrane was again gently washed with TBST for 20 min, three times. Then, the membrane was developed using the ECL chemiluminescence detection system (Beyotime P0018FS) and visualized with the ChemiDoc XRS+ system (Bio-Rad). Three independent experiments were conducted for reproducibility.

Monitoring c-di-GMP signal at the single-cell level

For measurements of c-di-GMP signaling, the validated reporter plasmid pCdrA-*gfp*, which produces green fluorescent protein (GFP) in response to an increase in c-di-GMP, was introduced into the experimental system. A 1000× diluted culture was inoculated into the apparatus described in the previous section and allowed to adhere to the surface for ~10 min, with the slight difference that the coverslips were not coated with poly-L-Lysine to avoid interference from background fluorescence. Bacteria were imaged using a Nikon Ti-E inverted microscope, which was equipped with an EMCCD camera (DU897, iXon3, Andor Technology). We used a 100× oil-immersion objective. Bacteria were illuminated with a 488-nm laser (Sapphire 488–200 mW, Coherent), using a standard GFP filter sets in the fluorescence imaging system with an exposure time of 500 ms. To ensure the consistency of culture and observation conditions, the data of wild-type and *cheY*-pME6032 carried strains were collected at the same time. More than 200 independent individuals of each strain were used for data analysis.

Single-cell c-di-GMP concentration was characterized by calculating fluorescence intensity. The average fluorescence intensity of a single cell was calculated by dividing the total fluorescence intensity of a single cell by the cell volume. Bacterial were simplified to a hollow cylindrical trunk with hollow hemispherical caps at both ends. The cell volume can be calculated by taking the length of the short axis of the cell body as the diameter of the sphere and the length of the long axis as the sum of the height of the cylinder and the diameter of the sphere. The mean fluorescence intensity of the cell was obtained by subtracting the average background fluorescence intensity from the total fluorescence intensity of the cell, and then dividing by the cell volume.

Acknowledgements

This work was supported by National Natural Science Foundation of China Grants (11925406, 12090053, 12304241, and 12304251), a Grant from the Ministry of Science and Technology of China (2019YFA0709303), Grants from the Natural Science Foundation of Shandong Province No. ZR2023QA111 and ZR2023QC168, a special Funding for High-level talents in the Medical and Health Industry in Jinan, a Grant from the Tai Shan Young Scholar Foundation of Shandong Province (tsqnz20231257) and the Science and Technology Development Program of Jinan Municipal Health Commission (2023-1-3).

Additional information

Author Contributions

J.Y. and R.Z. designed the work; Z.W., M.T. and S.F. performed the measurements with help from M.C.; Z.W and S.F analyzed the data; Z.W., J.Y. and R.Z. wrote the paper. Z.W., M.T. and S.F. contributed equally to this work.

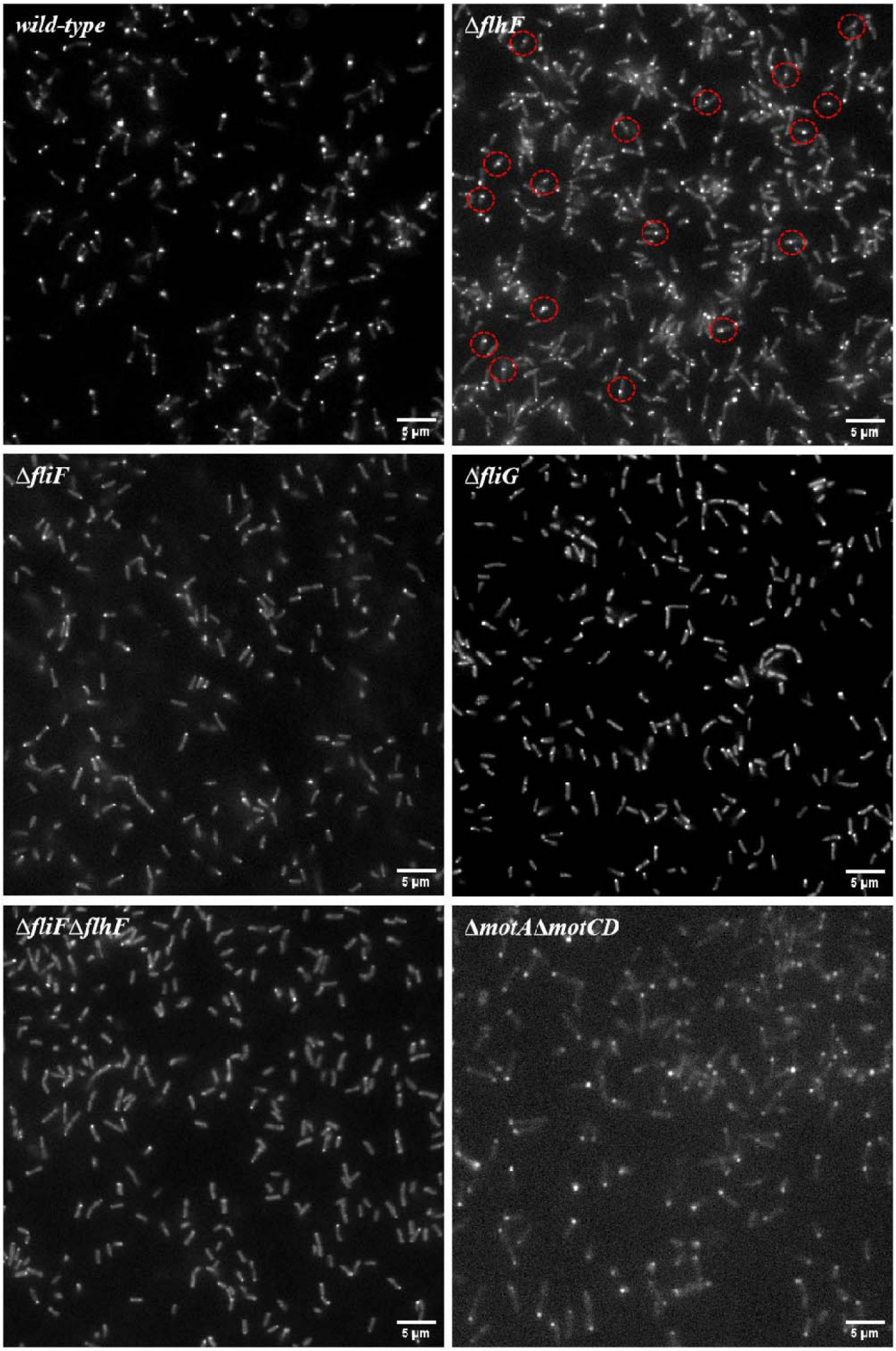

Fig. S1.

Distribution of chemotaxis complexes in multiple strains within representative large fields.

Red dotted circles indicate cells where the chemotaxis complex is located at the mid-cell position.

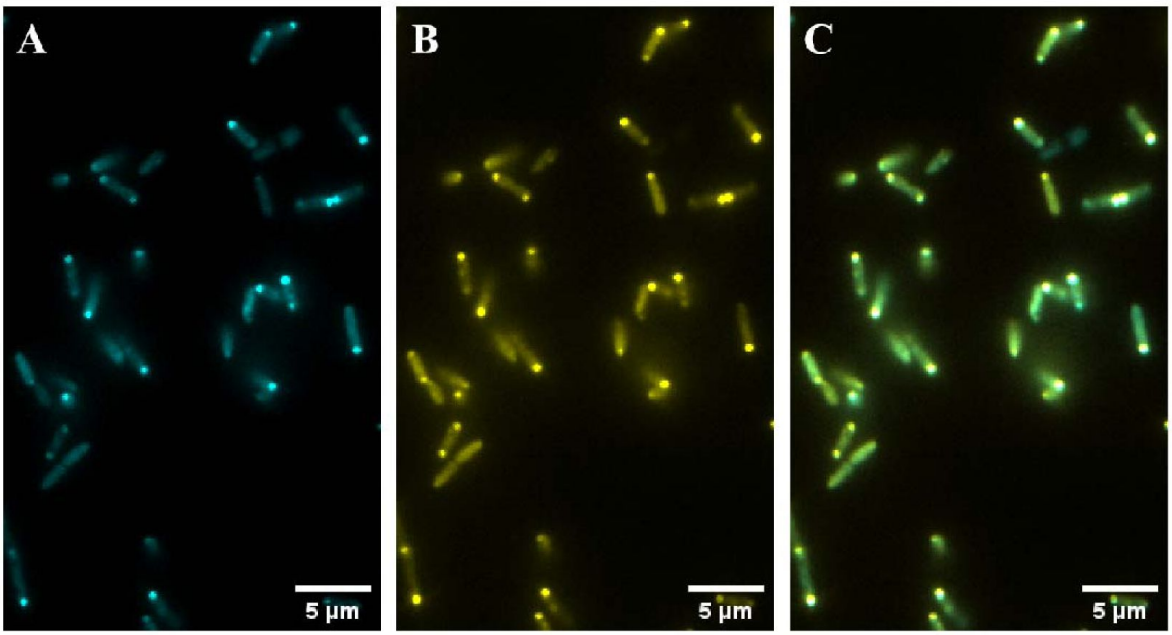

Fig. S2.

Co-localization of CheY-EYFP and CheA-ECFP in *P. aeruginosa*.

CheA-ECFP is shown in blue (left), CheY-EYFP in yellow (center), and the merged image is shown in the right panel.

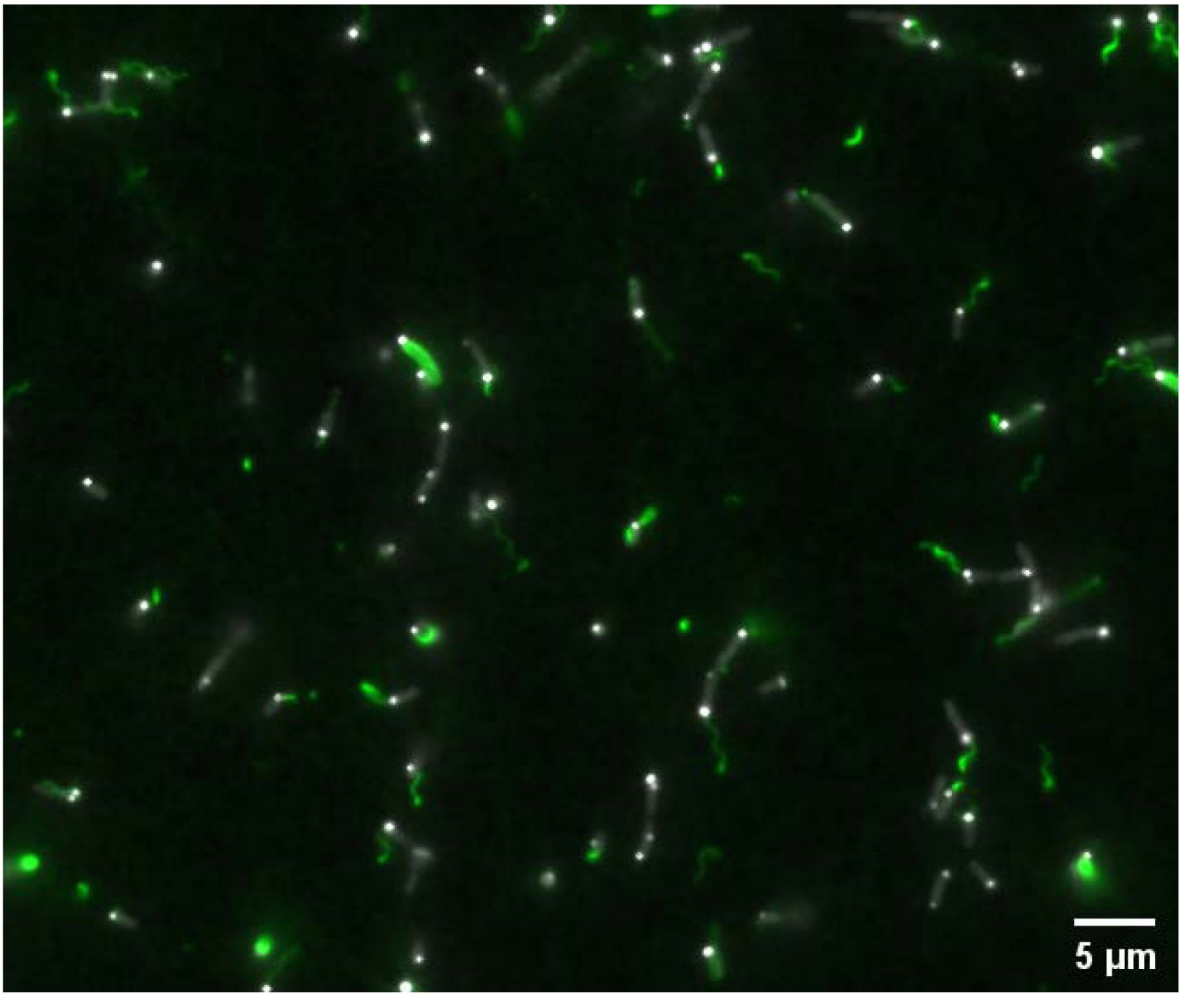

Fig. S3.

Simultaneous observation of the chemotaxis complex and flagellar filaments in the wild-type strain, shown in a representative large field.

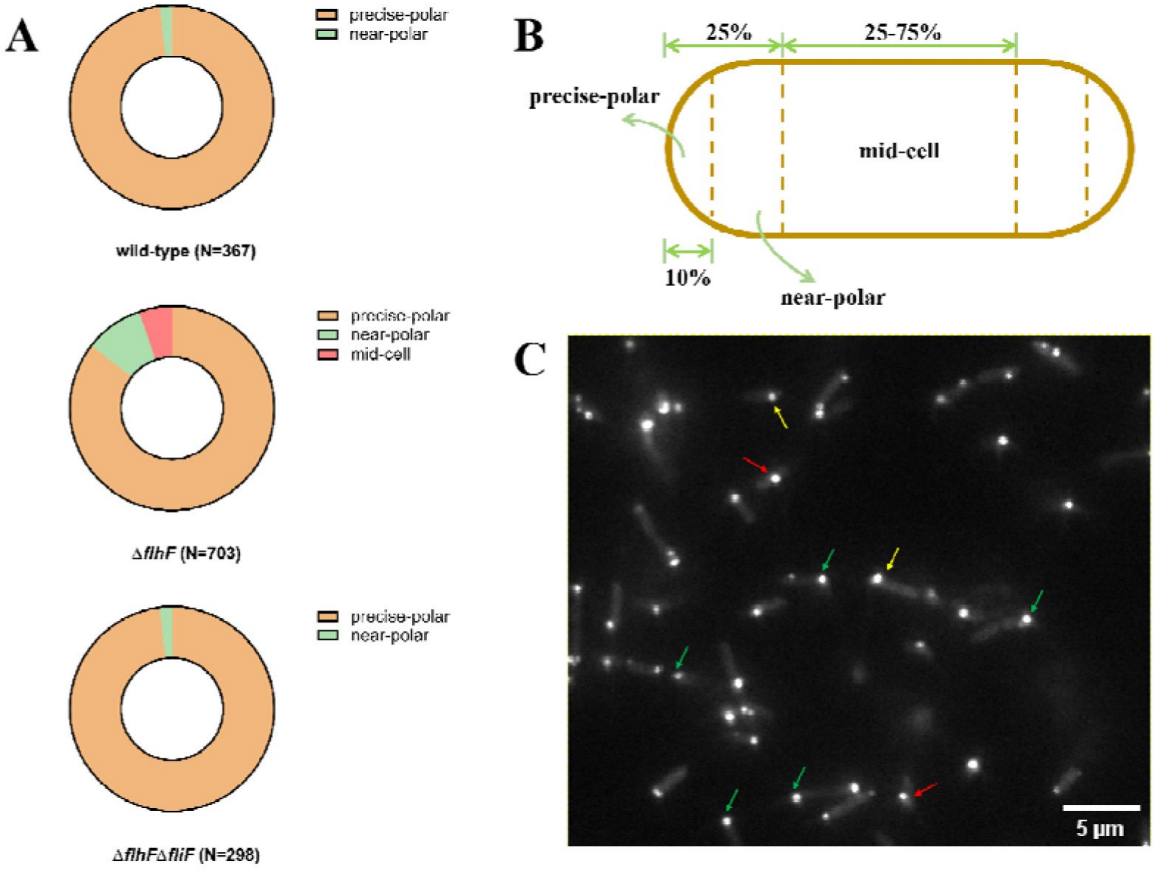

Fig. S4.

A. Distribution statistics of the chemotaxis complex in the wild-type strain and the *flhF* mutant. The distribution patterns are categorized into three types: precise-polar, near-polar, and mid-cell localization. In the wild-type strain, 98.1% of cells exhibit precise-polar localization of the chemotaxis complex, with the remainder showing near-polar distribution. In the *flhF* mutant, the proportion of cells with precise-polar localization decreases to 85.5%, and mid-cell localization appears in approximately 5% of cells. The *flhF-fliF* double mutant displays a distribution pattern similar to that of the wild-type strain. **B.** Schematic diagram of the classification of chemotactic complex locations. **C.** Cells with different chemotactic complex distribution patterns. Red arrows correspond to the mid-cell type, yellow arrows correspond to the near-polar type, and green arrows correspond to the precise-polar type.

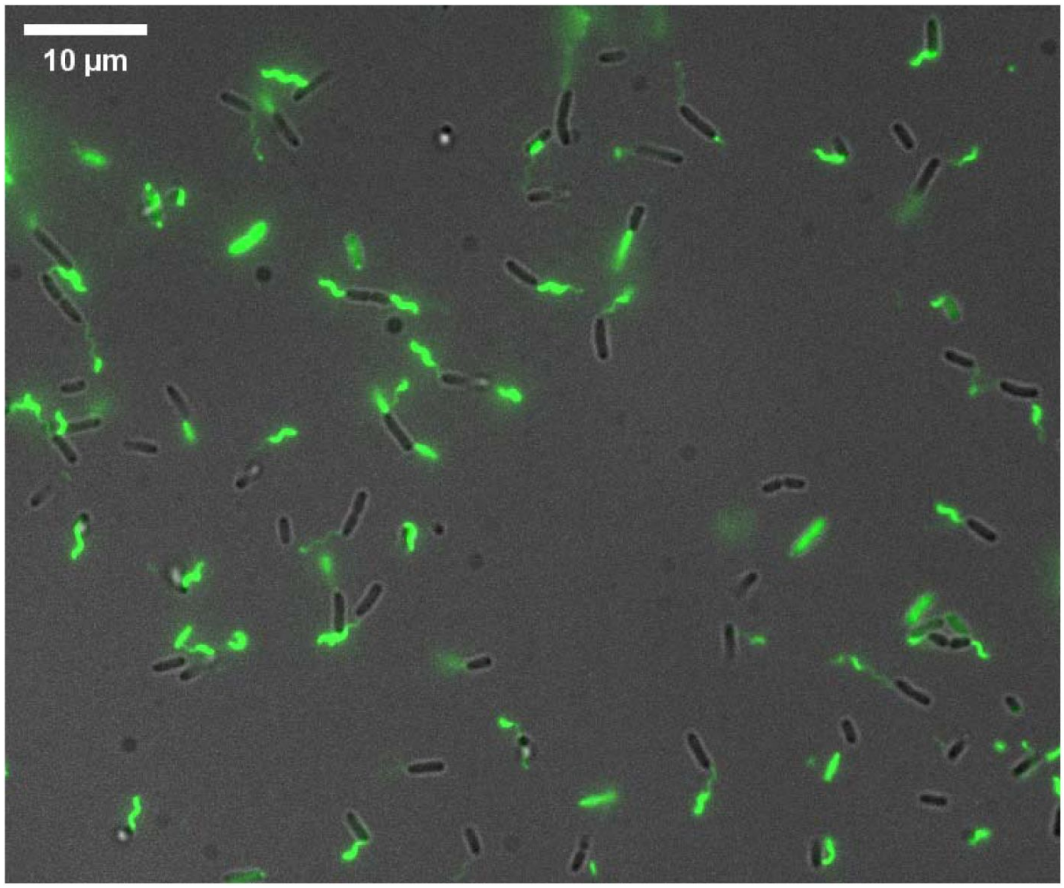

Fig. S5.

Knockout of *cheA* did not affect lagellar assembly efficiency of *P. aeruginosa*.

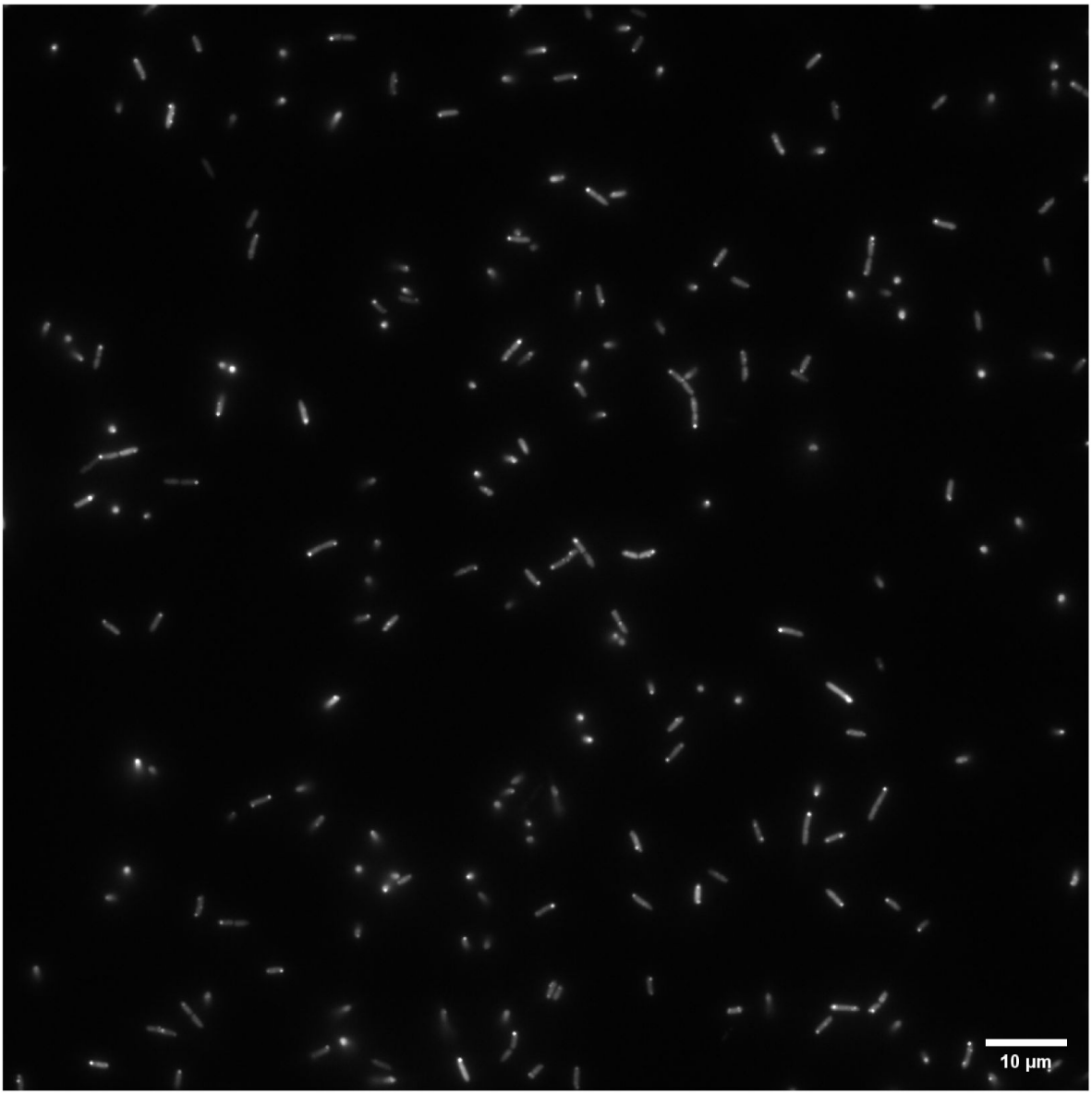

Fig. S6.

Localization of CheY-EYFP in the Δ*flgI* strain of *P. aeruginosa*.

The phenotype is similar to that of the wild-type strain.

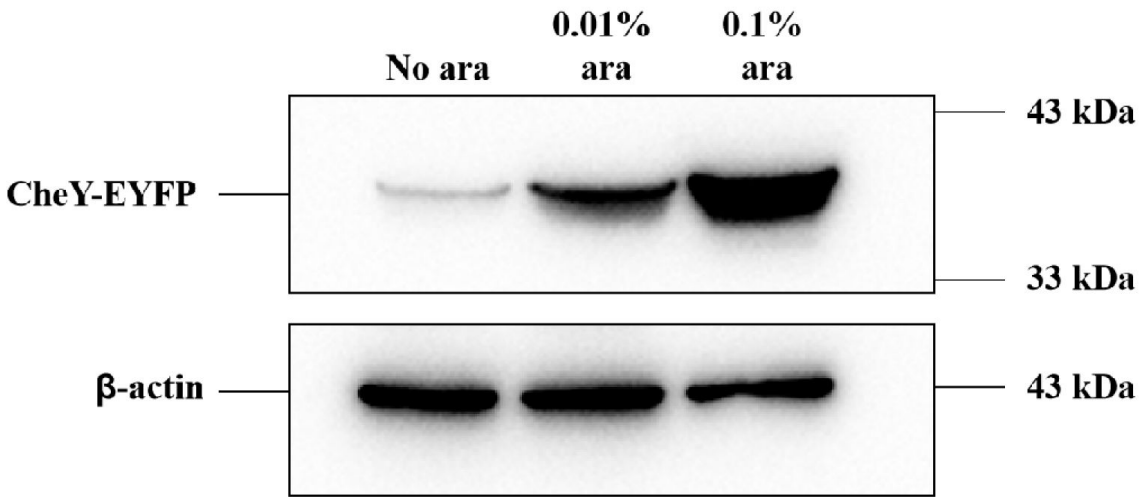

Fig. S7.

Intracellular CheY levels induced by different arabinose concentrations, measured by western blot analysis, showing clear differences across the concentration gradient.

β-actin was used as the housekeeping protein.

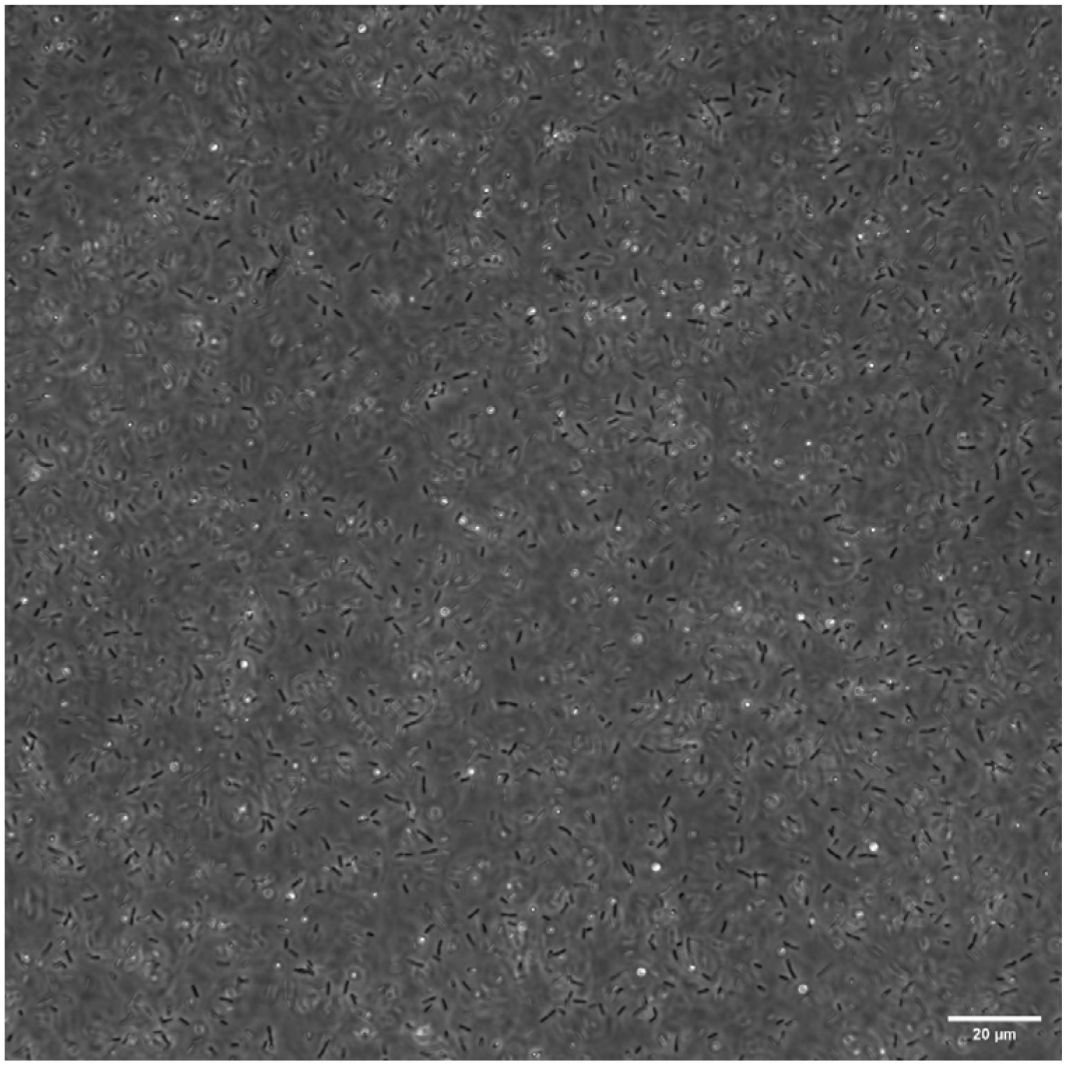

Fig. S8.

Co-overexpressing CheY and the phosphodiesterase (PDE) YhjH from *E. coli* mitigates cell aggregation caused by CheY overexpression in *P. aeruginosa*.

References

1 Halatek J., Brauns F., Frey E (2018) **Self-organization principles of intracellular pattern formation** *Philos. Trans. R. Soc. Lond. B Biol. Sci* **373**:20170107 Google Scholar

2 Thanbichler M., Shapiro L (2008) **Getting organized--how bacterial cells move proteins and DNA** *Nat. Rev. Microbiol* **6**:28–40 Google Scholar

3 Loose M., Kruse K., Schwille P (2011) **Protein self-organization: lessons from the min system** *Annu. Rev. Biophys* **40**:315–336 Google Scholar

4 Rothfield L., Taghbalout A., Shih Y. L (2005) **Spatial control of bacterial division-site placement** *Nat. Rev. Microbiol* **3**:959–968 Google Scholar

5 Fay A., Glickman M. S (2014) **An essential nonredundant role for mycobacterial DnaK in native protein folding** *PLoS Genet* **10**:e1004516 Google Scholar

6 Vaubourgeix J., et al. (2015) **Stressed mycobacteria use the chaperone ClpB to sequester irreversibly oxidized proteins asymmetrically within and between cells** *Cell Host Microbe* **17**:178–190 Google Scholar

7 Wang J., Brodmann M., Basler M (2019) **Assembly and Subcellular Localization of Bacterial Type VI Secretion Systems** *Annu. Rev. Microbiol* **73**:621–638 Google Scholar

8 Low H. H., et al. (2014) **Structure of a type IV secretion system** *Nature* **508**:550–553 Google Scholar

9 Briegel A., et al. (2012) **Bacterial chemoreceptor arrays are hexagonally packed trimers of receptor dimers networked by rings of kinase and coupling proteins** *Proc. Natl. Acad. Sci. U. S. A* **109**:3766–3771 Google Scholar

10 Zhang P., Khursigara C. M., Hartnell L. M., Subramaniam S (2007) **Direct visualization of Escherichia coli chemotaxis receptor arrays using cryo-electron microscopy** *Proc. Natl. Acad. Sci. U. S. A* **104**:3777–3781 Google Scholar

11 Cluzel P., Surette M., Leibler S (2000) **An ultrasensitive bacterial motor revealed by monitoring signaling proteins in single cells** *Science* **287**:1652–1655 Google Scholar

12 Sourjik V., Berg H. C (2002) **Binding of the Escherichia coli response regulator CheY to its target measured in vivo by fluorescence resonance energy transfer** *Proc. Natl. Acad. Sci. U. S. A* **99**:12669–12674 Google Scholar

13 Welch M., Oosawa K., Aizawa S., Eisenbach M (1993) **Phosphorylation-dependent binding of a signal molecule to the flagellar switch of bacteria** *Proc. Natl. Acad. Sci. U. S. A* **90**:8787–8791 Google Scholar

14 Schuhmacher J. S., Thormann K. M., Bange G (2015) **How bacteria maintain location and number of flagella?** *FEMS Microbiol Rev* **39**:812–822 Google Scholar

15 Jones C. W., Armitage J. P (2015) **Positioning of bacterial chemoreceptors** *Trends Microbiol* **23**:247–256 Google Scholar

16 Matilla M. A., Martin-Mora D., Gavira J. A., Krell T (2021) **Pseudomonas aeruginosa as a Model To Study Chemosensory Pathway Signaling** *Microbiol. Mol. Biol. Rev* **85**:e00151–120 Google Scholar

17 Guvener Z. T., Tifrea D. F., Harwood C. S (2006) **Two different Pseudomonas aeruginosa chemosensory signal transduction complexes localize to cell poles and form and remould in stationary phase** *Mol. Microbiol* **61**:106–118 Google Scholar

18 Amako K., Umeda A (1982) **Flagellation of Pseudomonas aeruginosa during the cell division cycle** *Microbiol. Immunol* **26**:113–117 Google Scholar

19 Schniederberend M., Abdurachim K., Murray T. S., Kazmierczak B. I (2013) **The GTPase activity of FlhF is dispensable for flagellar localization, but not motility, in Pseudomonas aeruginosa** *J. Bacteriol* **195**:1051–1060 Google Scholar

20 Murray T. S., Kazmierczak B. I (2006) **FlhF is required for swimming and swarming in Pseudomonas aeruginosa** *J. Bacteriol* **188**:6995–7004 Google Scholar

21 Greenfield D., et al. (2009) **Self-organization of the Escherichia coli chemotaxis network imaged with super-resolution light microscopy** *PLoS Biol* **7**:e1000137 Google Scholar

22 Thiem S., Sourjik V (2008) **Stochastic assembly of chemoreceptor clusters in Escherichia coli** *Mol. Microbiol* **68**:1228–1236 Google Scholar

23 Strahl H., et al. (2015) **Transmembrane protein sorting driven by membrane curvature** *Nat. Commun* **6**:8728 Google Scholar

24 Draper W., Liphardt J (2017) **Origins of chemoreceptor curvature sorting in Escherichia coli** *Nat. Commun* **8** Google Scholar

25 Koler M., Peretz E., Aditya C., Shimizu T. S., Vaknin A (2018) **Long-term positioning and polar preference of chemoreceptor clusters in E. coli** *Nat. Commun* **9**:4444 Google Scholar

26 Huitema E., Pritchard S., Matteson D., Radhakrishnan S. K., Viollier P. H (2006) **Bacterial birth scar proteins mark future flagellum assembly site** *Cell* **124**:1025–1037 Google Scholar

27 Ringgaard S., Schirner K., Davis B. M., Waldor M. K (2011) **A family of ParA-like ATPases promotes cell pole maturation by facilitating polar localization of chemotaxis proteins** *Genes Dev* **25**:1544–1555 Google Scholar

28 Ringgaard S., et al. (2014) **ParP prevents dissociation of CheA from chemotactic signaling arrays and tethers them to a polar anchor** *Proc. Natl. Acad. Sci. U. S. A* **111**:E255–E264 Google Scholar

29 Sourjik V., Berg H. C (2000) **Localization of components of the chemotaxis machinery of Escherichia coli using fluorescent protein fusions** *Mol. Microbiol* **37**:740–751 Google Scholar

30 Wu Z., Tian M., Zhang R., Yuan J (2021) **Dynamics of the Two Stator Systems in the Flagellar Motor of Pseudomonas aeruginosa Studied by a Bead Assay** *Appl Environ Microbiol* **87**:e0167421 Google Scholar

31 Tian M., Wu Z., Zhang R., Yuan J (2022) **A new mode of swimming in singly flagellated Pseudomonas aeruginosa** *Proc. Natl. Acad. Sci. U. S. A* **119**:e2120508119 Google Scholar

32 Altegoer F., Schuhmacher J., Pausch P., Bange G (2014) **From molecular evolution to biobricks and synthetic modules: a lesson by the bacterial flagellum** *Biotechnol Genet Eng Rev* **30**:49–64 Google Scholar

33 Kazmierczak B. I., Hendrixson D. R (2013) **Spatial and numerical regulation of flagellar biosynthesis in polarly flagellated bacteria** *Mol. Microbiol* **88**:655–663 Google Scholar

34 Minamino T., Imada K (2015) **The bacterial flagellar motor and its structural diversity** *Trends Microbiol* **23**:267–274 Google Scholar

35 Suzuki H., Yonekura K., Namba K (2004) **Structure of the rotor of the bacterial flagellar motor revealed by electron cryomicroscopy and single-particle image analysis** *J. Mol. Biol* **337**:105–113 Google Scholar

36 Minamino T., Imada K., Namba K (2008) **Molecular motors of the bacterial flagella** *Curr. Opin. Struct. Biol* **18**:693–701 Google Scholar

37 Levenson R., Zhou H., Dahlquist F. W (2012) **Structural insights into the interaction between the bacterial flagellar motor proteins FliF and FliG** *Biochemistry* **51**:5052–5060 Google Scholar

38 Hizukuri Y., Yakushi T., Kawagishi I., Homma M (2006) **Role of the intramolecular disulfide bond in FlgI, the flagellar P-ring component of Escherichia coli** *J. Bacteriol* **188**:4190–4197 Google Scholar

39 O'Connor J. R., Kuwada N. J., Huangyutitham V., Wiggins P. A., Harwood C. S (2012) **Surface sensing and lateral subcellular localization of WspA, the receptor in a chemosensory-like system leading to c-di-GMP production** *Mol. Microbiol* **86**:720–729 Google Scholar

40 Terasawa S., et al. (2011) **Coordinated reversal of flagellar motors on a single Escherichia coli cell** *Biophys J* **100**:2193–2200 Google Scholar

41 Sagawa T., et al. (2014) **Single-cell E. coli response to an instantaneously applied chemotactic signal** *Biophys J* **107**:730–739 Google Scholar

42 Segall J. E., Block S. M., Berg H. C (1986) **Temporal comparisons in bacterial chemotaxis** *Proc. Natl. Acad. Sci. U. S. A* **83**:8987–8991 Google Scholar

43 Qian C., Wong C. C., Swarup S., Chiam K. H (2013) **Bacterial tethering analysis reveals a "run-reverse-turn" mechanism for Pseudomonas species motility** *Appl Environ Microbiol* **79**:4734–4743 Google Scholar

44 Sourjik V (2004) **Receptor clustering and signal processing in E. coli chemotaxis** *Trends Microbiol* **12**:569–576 Google Scholar

45 Rybtke M. T., et al. (2012) **Fluorescence-based reporter for gauging cyclic di-GMP levels in Pseudomonas aeruginosa** *Appl Environ Microbiol* **78**:5060–5069 Google Scholar

46 Vaknin A., Berg H. C (2004) **Single-cell FRET imaging of phosphatase activity in the Escherichia coli chemotaxis system** *Proc. Natl. Acad. Sci. U. S. A* **101**:17072–17077 Google Scholar

47 Dasgupta N., et al. (2003) **A four-tiered transcriptional regulatory circuit controls flagellar biogenesis in Pseudomonas aeruginosa** *Mol. Microbiol* **50**:809–824 Google Scholar

48 Chilcott G. S., Hughes K. T (2000) **Coupling of Flagellar Gene Expression to Flagellar Assembly in Salmonella enterica Serovar Typhimurium and Escherichia coli** *Microbiol. Mol. Biol. Rev* **64**:694–708 Google Scholar

49 Beeby M., Ferreira J. L., Tripp P., Albers S.-V., Mitchell D. R (2020) **Propulsive nanomachines: the convergent evolution of archaella, flagella and cilia** *FEMS Microbiol Rev* **44**:253–304 Google Scholar

50 Kaplan M., et al. (2019) **The presence and absence of periplasmic rings in bacterial flagellar motors correlates with stator type** *eLife* **8**:e43487 https://doi.org/10.7554/eLife.43487 | Google Scholar

51 Kulasekara B. R., et al. (2013) **c-di-GMP heterogeneity is generated by the chemotaxis machinery to regulate flagellar motility** *eLife* **2**:e01402 https://doi.org/10.7554/eLife.01402 | Google Scholar

52. Kulasekara B. R. (2013) **Insight into a Mechanism Generating Cyclic di-GMP Heterogeneity in Pseudomonas aeruginosa PhD thesis** University of Washington Google Scholar

53 Zhou H., Rivas G., Minton A. P (2008) **Macromolecular crowding and confinement: biochemical, biophysical, and potential physiological consequences** *Annu. Rev. Biophys* **37**:375–397 Google Scholar

54 Cai Q., Li Z., Ouyang Q., Luo C., Gordon V. D (2016) **Singly Flagellated Pseudomonas aeruginosa Chemotaxes Efficiently by Unbiased Motor Regulation** *mBio* **7**:e00013–16 Google Scholar

55 Gibson D. G., et al. (2009) **Enzymatic assembly of DNA molecules up to several hundred kilobases** *Nat. Methods* **6**:343–345 Google Scholar

56 Hmelo L. R., et al. (2015) **Precision-engineering the Pseudomonas aeruginosa genome with two-step allelic exchange** *Nat. Protoc* **10**:1820–1841 Google Scholar

57 Turner L., Zhang R., Darnton N. C., Berg H. C (2010) **Visualization of Flagella during bacterial Swarming** *J. Bacteriol* **192**:3259–3267 Google Scholar

Author information

Zhengyu Wu*

Research Center of Translational Medicine, Central Hospital Affiliated to Shandong First Medical University, Jinan, China, Hefei National Research Center for Physical Sciences at the Microscale and Department of Physics, University of Science and Technology of China, Hefei,

China, Research Center of Translational Medicine, Jinan Central Hospital, Shandong University, Jinan, China

*These authors contributed equally

Maojin Tian*
Department of Critical Care Medicine, Zibo Central Hospital Affiliated to Binzhou Medical University, Zibo, China

*These authors contributed equally

Sanyuan Fu*
Hefei National Research Center for Physical Sciences at the Microscale and Department of Physics, University of Science and Technology of China, Hefei, China

*These authors contributed equally

Min Chen
Hefei National Research Center for Physical Sciences at the Microscale and Department of Physics, University of Science and Technology of China, Hefei, China

Rongjing Zhang
Hefei National Research Center for Physical Sciences at the Microscale and Department of Physics, University of Science and Technology of China, Hefei, China

For correspondence: rjzhang@ustc.edu.cn

Junhua Yuan
Hefei National Research Center for Physical Sciences at the Microscale and Department of Physics, University of Science and Technology of China, Hefei, China
ORCID iD: 0000-0002-6437-0655

For correspondence: jhyuan@ustc.edu.cn

Editors

Reviewing Editor
Ariel Amir
Weizmann Institute of Science, Rehovot, Israel

Senior Editor
Dominique Soldati-Favre
University of Geneva, Geneva, Switzerland

Reviewer #1 (Public review):

Summary:

The study by Wu et al presents interesting data on bacterial cell organization, a field that is progressing now, mainly due to the advances in microscopy. Based mainly on fluorescence microscopy images, the authors aim to demonstrate that the two structures that account for

bacterial motility, the chemotaxis complex and the flagella, colocalize to the same pole in Pseudomonas aeruginosa cells and to expose the regulation underlying their spatial organization and functioning.

Comments on revisions:

The authors have addressed all major and minor points that I raised in a satisfying way during the revision process. The work can now be regarded as complete: , the assumptions were clarified, the results are convincing, the conclusions are justified, and the novelty has been made clear. This manuscript will be of interest to cell biologists, mainly those studying bacteria, but not only

https://doi.org/10.7554/eLife.97514.3.sa3

Reviewer #2 (Public review):

Summary:

Here, the authors studied the molecular mechanisms by which the chemoreceptor cluster and flagella motor of Pseudomonas aeruginosa (PA) are spatially organized in the cell. They argue that FlhF is involved in localizing the receptors and motor to the cell pole, but a separate mechanism colocalizes them. Finally, the authors argue that the functional reason for this colocalization is to insulate chemotactic signaling from other signaling pathways, such as cyclic-di-GMP signaling.

Strengths:

The experiments and data are high quality. It is clear that the motor and receptors co-localize, and that elevated CheY levels lead to elevated c-di-GMP. The signaling crosstalk argument is plausible.

https://doi.org/10.7554/eLife.97514.3.sa2

Reviewer #3 (Public review):

Summary:

The authors investigated the assembly and polar localization of the chemosensory cluster in P. aeruginosa. They discovered that a certain protein (FlhF) is required for the polar localization of the chemosensory cluster while core motor structures are necessary for the assembly of the cluster. They found that flagella and chemosensory clusters always co-localize in the cell; either at the cell pole in wild type cells or randomly-located in the cell in FlhF mutant cells. They hypothesize that this co-localization is required to keep the level of another protein (CheY-P), which controls motor switching, at low levels as the presence of high-levels of this protein (if the flagella and chemosensory clusters were not co-localized) is associated with high-levels of c-di-GMP and cell aggregations.

Strengths:

The manuscript is clearly-written and straightforward. The authors applied multiple techniques to study the bacterial motility system including fluorescence light microscopy and gene editing. In general, the work enhances our understanding of the subtlety of interaction between the chemosensory cluster and the flagellar motor to regulate cell motility. This work will be of interest to bacteriologists and cell biologists in general.

https://doi.org/10.7554/eLife.97514.3.sa1

Author response:

The following is the authors' response to the previous reviews.

> ***Reviewer #1 (Public review):***
>
> *Summary:*
>
> *The study by Wu et al presents interesting data on bacterial cell organization, a field that is progressing now, mainly due to the advances in microscopy. Based mainly on fluorescence microscopy images, the authors aim to demonstrate that the two structures that account for bacterial motility, the chemotaxis complex and the flagella, colocalize to the same pole in Pseudomonas aeruginosa cells and to expose the regulation underlying their spatial organization and functioning.*
>
> *Comments on revisions:*
>
> *The authors have addressed all major and minor points that I raised in a satisfying way during the revision process. The work can now be regarded as complete, the assumptions were clarified, the results are convincing, the conclusions are justified, and the novelty has been made clear.*
>
> *This manuscript will be of interest to cell biologists, mainly those studying bacteria, but not only.*
>
> ***Reviewer #2 (Public review):***
>
> *Summary:*
>
> *Here, the authors studied the molecular mechanisms by which the chemoreceptor cluster and flagella motor of Pseudomonas aeruginosa (PA) are spatially organized in the cell. They argue that FlhF is involved in localizing the receptors-motor to the cell pole, and even without FlhF, the two are colocalized. Finally, the authors argue that the functional reason for this colocalization is to insulate chemotactic signaling from other signaling pathways, such as cyclic-di-GMP signaling.*
>
> *Strength:*
>
> *The experiments and data are high quality. It is clear that the motor and receptors co-localize, and that elevated CheY levels lead to elevated c-di-GMP.*
>
> *Weakness:*
>
> *The explanation for the functional importance of receptor-motor colocalization is plausible but is still not conclusively demonstrated. Colocalization might reduce CheY levels throughout the cell in order to reduce cross-talk with c-di-GMP. This would mean that if physiologically-relevant levels of CheYp near the pole were present throughout the cell, c-di-GMP levels would be elevated to a point that is problematic for the cell. Clearly demonstrating this seems challenging.*

We acknowledge that directly proving the necessity of colocalization to prevent problematic c-di-GMP elevation is experimentally challenging, as it would require creating a system where CheY-P is artificially distributed throughout the cell at physiologically relevant concentrations while maintaining normal chemotaxis function.

However, our data provide several lines of evidence supporting this model. First, we show that CheY overexpression leads to substantial c-di-GMP elevation (71.8% increase) and cell aggregation, demonstrating that elevated CheY levels can indeed cause problematic cross-

pathway interference. Second, previous work has shown that CheY-P levels near the pole are an order of magnitude higher than in the rest of the cell (ref. 46). If this elevated CheY-P concentration near the pole were present throughout the cell, our data suggest that c-di-GMP levels would be elevated sufficiently to cause cell aggregation (Fig. 4A), thereby disabling normal motility and chemotaxis. Third, the dose-dependent relationship between CheY concentration and aggregation phenotype supports the idea that precise spatial regulation of CheY levels is functionally important for avoiding cross-pathway interference.

> ***Reviewer #3 (Public review):***
>
> *Summary:*
>
> *The authors investigated the assembly and polar localization of the chemosensory cluster in P. aeruginosa. They discovered that a certain protein (FlhF) is required for the polar localization of the chemosensory cluster while a fully-assembled motor is necessary for the assembly of the cluster. They found that flagella and chemosensory clusters always co-localize in the cell; either at the cell pole in wild type cells or randomly-located in the cell in FlhF mutant cells. They hypothesize that this co-localization is required to keep the level of another protein (CheY-P), which controls motor switching, at low levels as the presence of high-levels of this protein (if the flagella and chemosensory clusters were not co-localized) is associated with high-levels of c-di-GMP and cell aggregations.*
>
> *Strengths:*
>
> *The manuscript is clearly written and straightforward. The authors applied multiple techniques to study the bacterial motility system including fluorescence light microscopy and gene editing. In general, the work enhances our understanding of the subtlety of interaction between the chemosensory cluster and the flagellar motor to regulate cell motility.*
>
> *Weaknesses:*
>
> *The major weakness for me in this paper is that the authors never discussed how the flagellar genes expression is controlled in P. aeruginosa. For example, in E. coli there is a transcriptional hierarchy for the flagellar genes (early, middle, and late genes, see Chilcott and Hughes, 2000). Similarly, Campylobacter and Helicobacter have a different regulatory cascade for their flagellar genes (See Lertsethtakarn, Ottemann, and Hendrixson, 2011). How does the expression of flagellar genes in P. aeruginosa compare to other species? how many classes are there for these genes? is there a hierarchy in their expression and how does this affect the results of the FliF and FliG mutants? In other words, if FliF and FliG are in class I (as in E. coli) then their absence might affect the expression of other later flagellar genes in subsequent classes (i.e., chemosensory genes). Also, in both FliF and FliG mutants no assembly intermediates of the flagellar motor are present in the cell as FliG is required for the assembly of FliF (see Hiroyuki Terashima et al. 2020, Kaplan et al. 2019, Kaplan et al. 2022). It could be argued that when the motor is not assembled then this will affect the expression of the other genes (e.g., those of the chemosensory cluster) which might play a role in the decreased level of chemosensory clusters the authors find in these mutants.*

We thank the reviewer for the valuable suggestions. In the revised manuscript, we have further elaborated on the regulatory control of flagellar genes expression in P. aeruginosa (see our response to comment #4).

> *Comments on revisions:*

> *I believe the authors have performed additional experiments that improved their manuscript and they have answered many of my comments and those of the other reviewers. I am supportive of publishing this manuscript, but I still find the following points that are not clear to me (probably I am misunderstanding some points; the authors can clarify).*
>
> *(1) In response to reviewer 1, the authors say that they "analyzed and categorized the distribution of the chemotaxis complex in both wild-type and flhF mutant strains into three patterns: precise-polar, near-polar, and mid-cell localization." I can see what they mean by polar and mid-cell, but near-polar sounds a bit elusive? Can they provide examples of this stage and mention how accurately they can identify it? Also, do the pie charts they show in Figure S4 really show "significant alterations"? There is a difference between 98% and 85% as they mention in their response to reviewer 1, but I am not sure that this is significant? Probably they can explain/change the language in the text? Also, the number of cells they counted for FlhF mutant is more than the double of other strains (WT and FlhF FliF mutant)?*

We thank the reviewer for the valuable suggestions. To clarify, we divided the intracellular area along the cell's long axis into three domains: the two ends each representing 10% of the length as the precise-polar domain, the central 50% as the mid-cell domain, and the remaining regions between these as the near-polar domain. The localization pattern of the chemotaxis complex was assigned based on the position of the fluorescence intensity centroid within these domains.

Regarding the significance of the changes, you are correct to question our language. When flhF was knocked out, the proportion of chemotaxis complexes with precise-polar distribution decreased from 98% to 85% - a 13% reduction. While this represents a measurable shift in localization pattern, describing this as "significant alterations" was probably imprecise. We have revised this language to more accurately reflect the magnitude of the change (lines 169-177).

For the cell counting, we increased the sample size for the flhF mutant because this strain exhibited the appearance of mid-cell localization (approximately 5% of cells), which was not observed in wild-type or flhF fliF double mutant strains. To accurately quantify this rare phenotype and ensure statistical reliability, we analyzed more cells for this particular strain. This explains why the flhF mutant dataset contains approximately double the number of cells compared to the other strains.

We have redrawn Figure S4 to include a clear schematic diagram of the cell partitioning method and provided representative examples of each localization pattern (precise-polar, near-polar, and mid-cell) to better illustrate how we distinguished between these categories.

> *(2) One thing that also confused me is the following: One point that the authors stress is that FlhF localizes both the flagellum and the chemoreceptors to the pole. However, if I look at Figure 2B, the flagellum and the chemoreceptors still co-localize together (although not at the pole). If FlhF was responsible for co-localizing both of them to the pole, then wouldn't one expect them to be randomly localized in this mutant and by that I mean that they do not co-localize but that each of them (the flagellum and the chemoreceptors) are located in a different random location of the cell (not co-localized). The fact that they are still co-localized together in this mutant could also be interpreted by, for example, that FlhF localizes the flagellum to the pole and another mechanism localizes the chemoreceptors to the flagellum, hence, they still co-localize in this mutant because the chemoreceptors follow the flagellum by another mechanism to wherever it goes?*

Thank you for this insightful observation. You are correct that our current experimental results do not definitively establish that FlhF directly localizes both the flagellum and chemoreceptors to the pole independently. The persistent colocalization of flagella and chemoreceptors in the DflhF mutant, even when both are mislocalized away from the pole, actually suggests a more complex regulatory mechanism than we initially proposed.

This observation highlights an important distinction between polar targeting and colocalization maintenance. Our data suggest that FlhF influences the polar targeting of the flagellum-chemoreceptor assembly, but the colocalization itself appears to be governed by a different mechanism that operates independently of FlhF. This could involve direct protein-protein interactions between flagellar and chemotaxis components, or shared assembly machinery that we have yet to identify.

To better reflect this interpretation, we have revised the subsection title (line 150). We have also modified the relevant discussion (line 180) to more accurately describe FlhF's role in polar targeting rather than claiming it directly controls chemoreceptor localization.

> *(3) In the response to reviewers, the authors mention "suggesting that the assembly of the receptor complex is likely influenced mainly by the C-ring and MS-ring structures rather than by the P ring". However, in the article, they still write "The complete assembly of the motor serves as a partial prerequisite for the assembly of the chemotaxis complex, and its assembly site is also regulated by the polar anchor protein FlhF" despite their FlgI results which is not in accordance with this statement? Also, As I mentioned in my previous report, in FliG and FliF mutant the motor does not assemble (see Hiroyuki Terashima et al. 2020., and Kaplan et al., 2022).*

We thank the reviewer for the suggestions and acknowledge the contradictions in our original text. You are correct that in DfliF and DfliG mutants, the flagellar motor does not assemble, while the P ring (FlgI) functions as a bushing for the peptidoglycan layer and its absence does not prevent motor assembly.

Our DflgI results, which showed normal chemotaxis complex assembly similar to wild-type, clearly demonstrate that the P ring is not required for chemoreceptor complex formation. This contradicts our original statement that "complete assembly of the motor serves as a partial prerequisite for the assembly of the chemotaxis complex."

We have corrected this inconsistency by: 1) Revising the subsection title (line 186) to more accurately reflect that core motor structures, rather than complete motor assembly, influences chemoreceptor complex formation. 2) Modifying sentences in the introduction (lines 97-98) to better align with our experimental findings.

> *(4) The authors have said in their response to my point "and currently, there is no evidence that FliA activity is influenced by proteins like FliG". I just want to clarify what I meant in my previous report: In E. coli, FliA binds to FlgM, and when the hook is assembled FlgM is secreted outside the cell allowing FliA to trigger the transcription of class III genes, which include the chemosensory genes (see Figure 5 in Beeby et al, 2020 in FEMS Microbiology, and Chilcott and Hughes, 2000). This implies that if the hook is not built, then late genes (including the chemoreceptors) should not be present. However, in Kaplan et al., 2019, the authors imaged a FliF mutant in Shewanella oneidensis (Figure S3) and still saw that chemoreceptors are present (I believe the authors must highlight this). This suggests that species such as Shewanella and Pseudomonas have a different assembly process than that E. coli, and although the authors say that in the text, I believe they still can refine this part more in the spirit of what I wrote here.*

We thank the reviewer for the important clarification regarding the differences in transcriptional regulation among bacterial species. We agree that the observation of chemoreceptors in Shewanella oneidensis DfliF mutants (Kaplan et al., 2019) represents a significant deviation from the well-characterized E. coli model and merits stronger emphasis. In response, we have expanded the discussion to more clearly highlight the critical distinctions in the transcriptional regulatory circuits governing flagellar and chemoreceptor biogenesis between E. coli and species such as Shewanella oneidensis and Pseudomonas aeruginosa (lines 351-363).

> *I do not like to ask for additional experiments in the second round of review, so for me if the authors modify the text to tackle these points and allow for probable alternative explanations/ highlight gaps/ modify language used for some claims, then that is fine with me.*
>
> ***Reviewer #2 (Recommendations for the authors):***
>
> *It is plausible that colocalization reduces CheY levels throughout the cell in order to reduce cross-talk with c-di-GMP. This would mean that if physiologically-relevant levels of CheYp near the pole were present throughout the cell, c-di-GMP levels would be elevated to a point that is problematic for the cell. Clearly demonstrating this seems challenging.*

We acknowledge that directly proving the necessity of colocalization to prevent problematic c-di-GMP elevation is experimentally challenging, as it would require creating a system where CheY-P is artificially distributed throughout the cell at physiologically relevant concentrations while maintaining normal chemotaxis function.

However, our data provide several lines of evidence supporting this model. First, we show that CheY overexpression leads to substantial c-di-GMP elevation (71.8% increase) and cell aggregation, demonstrating that elevated CheY levels can indeed cause problematic cross-pathway interference. Second, previous work has shown that CheY-P levels near the pole are an order of magnitude higher than in the rest of the cell (ref. 46). If this elevated CheY-P concentration near the pole were present throughout the cell, our data suggest that c-di-GMP levels would be elevated sufficiently to cause cell aggregation (Fig. 4A), thereby disabling normal motility and chemotaxis. Third, the dose-dependent relationship between CheY concentration and aggregation phenotype supports the idea that precise spatial regulation of CheY levels is functionally important for avoiding cross-pathway interference.

https://doi.org/10.7554/eLife.97514.3.sa0